

THE UNIVERSITY OF HULL

**Development of a Portable Microfluidic System
for Monitoring Ions River Water**

being a Thesis submitted for the degree of
MSc. Chemistry

in the University of Hull

by

Chee Keong, Ong
BSc (University of Hull)

March 2012

Abstract

Nowadays, there is a growing demand for predictive models that are capable of predicting future trends in water quality which is constantly being affected by environmental changes and industrialisation. The presence of various nutrient contaminants in surface water poses a serious threat to human health. The initial step for the development of this predictive model is to have an *in situ* monitoring system that provides high frequency screening and monitoring of nutrients in surface water. At present, the conventional *in situ* monitoring systems available are too cumbersome, expensive and laborious.

The main aim of this project was to develop a portable and automated miniaturised total analytical system (μ TAS) monitoring system that could provide *in situ* river water nutrient measurements over a wide range of analytes such as cations (Na^+ , K^+ , Ca^{2+} , Mg^{2+} , NH_4^+) and anions (Cl^- , NO_2^- , NO_3^- , SO_4^{2-} , PO_4^{3-}). The contribution of this work to the overall project was to integrate sample pre-treatment procedures on-chip to allow direct and reproducible analysis of real samples and to investigate the possibility of fabricating an anion exchange column through immobilisation with different ion exchangers using a self-fabricated silica monolithic column.

A combination of on-chip sample filtration and sample introduction system was investigated using potassium silicate frit and electrophoretic injection to selectively extract the analytes prior to introduction into the microfluidic system. The frits were optimised and proven to possess high mechanical stability and flow resistance against hydrodynamic and hydrostatic flows. Sodium ions were successfully migrated into the microfluidic system through the frit by electrophoretic flow with ion migration efficiency of 26%. Despite the low ion migration efficiency obtained, the results demonstrated the potential of coupling the sample filtration frit with sample introduction system in a microfluidic chip to prevent passage of large particulates into the system causing system blockage.

Isotachopheresis (ITP) is one of the most widely reported on-chip sample pre-concentration techniques but due to the complexity of the ternary buffer systems in ITP, introduction of these buffers in an appropriate and cost-effective approach would be

difficult. An investigation of a simple miniaturised gel supported ITP system was conducted where all the necessary buffers were encapsulated in agarose gel and pre-loaded onto a microfluidic chip. A proof of principle experiment was conducted in a “goal post” system and sodium ions were shown to be able to migrate through the gel encapsulated buffer system. However, implementation of the experiment in the microfluidic chip was unsuccessful due to occurrence of gel deformation.

Preliminary investigation of fabricating an anion exchange column using a self-fabricated silica monolithic column was conducted based on solid phase extraction (SPE). Two different ion exchangers, chitosan and lysine, were investigated due to their high content of amino groups. Lysine was shown to be successfully immobilised onto the silica surface and to have reasonable extraction efficiency of 62% in extracting nitrate ions. Chitosan, however, failed to show any positive result, this may be due to an unsuccessful functionalisation procedure or poor pre-conditioning of the column.

The findings obtained in this thesis contributed to the main aim of the project by demonstrating the potential of coupling a sample filtration frit with a sample introduction system which allowed the *in situ* μ TAS monitoring system to extract the analytes from the sample matrix prior to introduction into the system. This is crucial as these real samples contain large particulates that can cause serious operational problems such as system blockage. In addition, due to the high cost of commercial silica monolithic exchange column, the work presented indicated the potential for self-fabricating the ion exchange silica monolithic column, which is more cost-effective.

Acknowledgements

I would like to thank my supervisors, Professor Gillian Greenway and Professor Steve Haswell for their continued support and guidance throughout my whole master programme.

I would also like to thank the members of “Linking Improved Modelling of Pollution to Innovative Development of Sensors (LIMPIDS)” group namely Dr. Ian Bell, Amy Webster, Etienne Joly and David Ingles who have contributed time, knowledge and support.

I would like to extend my gratitude to Dr. Kirsty Shaw and Dr. Ping He for all their support and advice during my time in the laboratory. I also wish to express thanks to Asim Jilani for his help on functionalisation of silica monoliths.

I would thank all the staff and research students of the Analytical group for all their help and advice throughout the duration of my time in the university.

Last but not least, I am thankful to my family for their love, moral and financial support throughout my studies, especially my mum and my partner, Pui Mei.

List of Abbreviations

μ TAS	micro total analytical system
CEC	capillary electrochromatography
EOF	electro osmotic flow
EP	electrophoretic flow
FASS	field amplified sample stacking
GPTMS	3-glycidopropyltrimethoxysilane
HEC	hydroxyethylcellulose
IC	ion chromatography
ITP	isotachopheresis
LE	leading electrolyte
LOC	lab-on-a-chip
PEO	polyethylene oxide
SPE	solid phase extraction
TAS	total analysis system
TE	terminating electrolyte
TEOS	tetraethoxysilane
TRIS	tris(hydroxymethyl) aminomethane

List of Figures

Figure 1.1: Formation of Helmholtz double layers	7
Figure 1.2: EOF in the opposite direction of electrophoretic flow of anions	8
Figure 1.3: The design of H-filter	11
Figure 1.4: Formation of discrete zones between LE and TE	13
Figure 1.5: Schematic diagram of basic components of an ion chromatograph	17
Figure 1.6: SEM image of a silica monolith fabricated through sol-gel method	21
Figure 2.1: The potassium silicate frit made in the capillary	28
Figure 2.2: The potassium silicate frit made in the microfluidic chip	29
Figure 2.3: The “goal post” system for hydrodynamic pressure resistance test	30
Figure 2.4: The microfluidic chip for hydrodynamic pressure resistance test	30
Figure 2.5: The “goal post” setup for EOF suppressed electrophoretic system	32
Figure 2.6: Contactless conductivity detector	32
Figure 2.7: The setup for electrophoretic system in microfluidic chip	33
Figure 2.8: The calibration curve for sodium ions for unsuppressed EOF system	41
Figure 2.9: The calibration curve for sodium ions for suppressed EOF system	43
Figure 2.10: The calibration curve for sodium ions for suppressed EOF system	47
Figure 2.11: The calibration curve for the contactless conductivity detector	50
Figure 2.12: Conductivity changes recorded by contactless conductivity detector	51

Figure 3.1: The “goal post” system for ITP with gel encapsulated buffer system	58
Figure 3.2: Schematic showing the design of the microfluidic chip for ITP	59
Figure 4.1: In house fabricated silica monolithic column	69
Figure 4.2: The chromatogram for 7 anions standard analysis by Dionex IC	74
Figure 4.3: The ion chromatogram for acetate buffer pH 4 (activation buffer)	75
Figure 4.4: The ion chromatogram for tris-acetate buffer pH 8.6 (elution buffer)	75
Figure 4.5: The ion chromatogram for sample of 5 mM NaNO ₃ in acetate buffer	76

List of Tables

Table 2.1: Comparison of different frit compositions ratios	35
Table 2.2: Comparison of different oven temperature and incubation time	36
Table 2.3: Comparison of permanent surface modification and dynamic coating	38
Table 2.4: The results under electrokinetic flow in “goal post” system	42
Table 2.5: The results under electrophoretic flow in “goal post” system	44
Table 2.6: The results of diffusion test in “goal post” system	45
Table 2.7: The results under electrophoretic flow in microfluidic chip	48
Table 3.1: Resistance of agarose gel rod with different electrolytes concentration	61
Table 3.2: Concentration of sodium in sample after ITP in “goal post” system	62
Table 3.3: Resistance of the agarose gel rod after ITP in “goal post” system	63
Table 4.1: Recovery of nitrate using chitosan-functionalised silica monolith	77
Table 4.2: Recovery of nitrate using lysine-functionalised silica monolith	78

Table of Contents

Abstract	ii
Acknowledgements	iv
List of Abbreviations	v
List of Figures	vi
List of Tables	viii
Table of Contents	ix
Chapter 1 Introduction	1
1.1 Background and Introduction	2
1.1.1 Conventional monitoring techniques	3
1.2. Introduction to microfluidic chip and miniaturised total analytical systems (μ TAS)	4
1.3. Sample introduction in microfluidic system	5
1.3.1 Electrokinetic injection	5
1.3.2 Hydrodynamic injection	6
1.3.3 Theory of electrokinetic	7
1.3.3.1 Electro-osmotic flow (EOF)	7
1.3.3.2 Electrophoretic flow	8

1.4	Sample pre-treatment in microfluidic system	9
1.4.1	Extraction or clean-up of analyte of interest from sample matrix	10
1.4.2.	Sample pre-concentration	12
1.4.2.1	Field amplified sample stacking (FASS)	12
1.4.2.2	Isotachopheresis (ITP)	13
1.4.2.3	Solid phase extraction (SPE)	15
1.5	Separation techniques in microfluidic system for water monitoring	16
1.6	Background of ion chromatography	17
1.6.1.	Ion chromatography system	17
1.6.2.	Common applications of IC in water analysis	19
1.6.3	Advances in separation process of IC	20
1.7	Monoliths	20
1.8	Aims and Objectives	24
Chapter 2	On-Chip Sample Introduction System with Filtration Mode	25
2.1	Introduction	26
2.2.	Experimental	27
2.2.1	Instrumentation	27
2.2.2	Chemicals and Materials	27
2.2.3	Fabrication of potassium silicate frit in the capillary and microfluidic chip	28
2.2.4	Mechanical stability and flow resistance tests for potassium silicate frit in capillary and microfluidic chip	29

2.2.5	Preparation of hydroxyethylcellulose (HEC) solution for EOF suppression	31
2.2.6	Investigation for the introduction of ions through the frit in “goal post” system using electrophoretic flow	31
2.2.7	Investigation for the ion diffusion through the frit	33
2.2.8	Investigation for the introduction of ions through the frit in a microfluidic chip using electrophoretic flow	33
2.3	Results and Discussion	34
2.3.1	Optimisation of experimental parameters for fabrication of frit	34
2.3.1.1	Frit composition ratio	35
2.3.1.2	Oven temperature and incubation time	36
2.3.2	EOF suppression	37
2.3.3	Selection of buffer	40
2.3.4	Electrokinetic injection of sodium ions through frit in capillary in “goal post” system	41
2.3.5	Preparation of potassium silicate frit in a microfluidic chip	46
2.3.6	Electrophoretic injection of sodium ions through frit in a microfluidic chip	47
2.3.7	Development of a contactless conductivity detector	49
2.3.8	Conclusion	53

Chapter 3	Sample pre-concentration with miniaturised isotachophoresis	54
3.1	Introduction	55
3.2	Experimental	56
3.2.1	Instrumentation	56
3.2.2	Chemicals and Materials	56
3.2.3	Encapsulation of leading electrolyte (LE) and terminating electrolyte (TE) in agarose gel for ITP in “goal post” system	57
3.2.4	Encapsulation of leading electrolyte (LE) and terminating electrolyte (TE) in agarose gel for ITP in microfluidic chip	57
3.2.5	Preliminary investigation of ITP using agarose encapsulated electrolytes buffer system in “goal post” system	58
3.2.6	Preliminary investigation of ITP using agarose encapsulated electrolytes buffer system in a microfluidic chip	59
3.3	Results and Discussion	60
3.3.1	Optimisation of the agarose gel rod containing leading and terminating electrolytes	60
3.3.1.1	Agarose gel concentration	60
3.3.1.2	Resistance (Ω) of the agarose gel	60
3.3.2	Investigation of ITP using agarose encapsulated electrolytes buffer system in “goal post” system for sodium ions	62
3.3.3	Miniaturised ITP in agarose encapsulated electrolytes buffer system in microfluidic chip.	64
3.3.4	Conclusion	65

Chapter 4	Functionalisation of Silica Monoliths for Ions Separation	66
4.1	Introduction	67
4.2	Experimental	68
4.2.1	Instrumentation	68
4.2.2	Chemicals and Materials	68
4.2.3	Fabrication of sol-gel TEOS silica monolith	69
4.2.4	Functionalisation of silica monoliths with chitosan	70
4.2.5	Functionalisation of silica monoliths with lysine	71
4.2.6	Investigation of functionalised silica monolith as anion exchange column	71
4.3	Results and Discussion	73
4.3.1	Anion sample selection for investigation of functionalised silica monolith	73
4.3.2	Method selection for investigation of functionalised silica monolith	73
4.3.3	Analysis of the solid phase extraction buffer system	74
4.3.4	Investigation of solid phase extraction of nitrate ions by chitosan-functionalised silica monolith	77
4.3.4.1	Optimisation of chitosan concentration for functionalisation	77
4.3.4.2	Investigation of SPE using chitosan-functionalised silica monolith	77
4.3.4.3	Investigation of SPE of nitrate ions by lysine- functionalised silica monolith	78
4.3.5	Conclusion	79

Chapter 5	Conclusion and Future Work	80
5.1	The application of μ TAS for <i>in situ</i> river water monitoring	81
5.2	On-chip sample introduction system with filtration mode	82
5.3	Sample pre-concentration with miniaturised isotachopheresis	83
5.4	Functionalisation of silica monoliths for ions separation	84
Chapter 6	References	85

Chapter 1 Introduction

1.1 Background and Introduction

In recent years, the quality of surface water is becoming one of the major concerns worldwide due to the widespread problem of water pollution. In particular, the presence of nutrient contaminants in water as a result of environmental change is affecting the water quality. These nutrient contaminants are harmful to humans when present above the Maximum Contaminant Limit (MCL).¹

Nitrate ions, one of the major nutrient contaminants, which are derived from the utilisation of fertiliser or pesticides in agricultural areas, are shown to cause serious illness known as infantile cyanosis in infants, which is fatal if untreated.^{2,3} In addition, it has also been found that nitrate and phosphorus are the substances that contribute to eutrophication and toxic algal blooms, which eventually cause threat to certain aquatic organisms.⁴ On top of that, Berenzen *et al.* found that nitrite and ammonia, which are the products of ammonium, are very toxic to macroinvertebrates.⁵ Additionally, calcium and magnesium are also well known to be the causes of water hardness.

Therefore, there is an increased demand for development of a predictive model that could forecast future changes in water quality. Currently, a few predictive models have been developed, which are able to predict the effects of environmental changes. However these models failed to predict the future trends in water quality due to lack of detailed and constant environmental measurements. Hence, in the early stages of developing the predictive model, an innovative measurement system was required to constantly monitor and measure the chemical changes in surface water effectively.⁶

1.1.1 Conventional monitoring techniques

Traditional chemical monitoring techniques involve laborious procedures where samples are collected in the field and transported back to the laboratory for analysis. Besides requiring considerable effort and expense, the long period of delay between sample collection and analysis allows changes in samples and contamination which leads to inaccurate results. There has been extensive research carried out with the aim of developing an *in situ* monitoring system to overcome the problem of sample transportation. Chemical sensors such as electrochemical electrodes have been developed for direct detection of pollution allowing *in situ* monitoring. Unfortunately, these chemical sensors have several disadvantages, such as requiring frequent recalibrations, lack of durability and being limited by selectivity.⁷

On the other hand, total analysis systems (TAS) such as flow injection analysis (FIA) and sequential injection analysis (SIA) have been developed to allow *in situ* chemical analysis.^{8,9} Currently, there are a few systems which have been successfully commercialised. Even though the systems commercially available today provide *in situ* and high speed analysis, the systems are generally large in size, heavy, expensive and involve large consumption of reagents.^{10,11} These limitations have inspired a number of investigations into developing a fast, robust and sensitive and yet cost effective μ TAS *in situ* monitoring system.

1.2. Introduction to microfluidic chip and miniaturised total analytical systems (μ TAS)

A microfluidic chip is a miniaturised analytical platform containing a network of micron dimension channels. This device, which is usually made of glass, polymeric materials or silicon, allows the manipulation of liquid in microlitre volumes.¹²

Miniaturised total analytical systems (μ TAS) or lab-on-a-chip (LOC) devices are miniaturised analysis systems that integrate all the chemical analysis functions, such as sample injection, sample pre-treatment, separation and detection onto a single microfluidic device. The idea of miniaturising an analysis system was first introduced by Terry *et al.* in 1979, when a gas chromatograph was fabricated on a silicon wafer.¹³ It was further improved by Manz *et al.* in 1990, when the concept of “micro total analytical system (μ TAS)” was proposed. An open-tubular liquid chromatography separation column and platinum electrode detector were successfully integrated onto one microfluidic chip.¹⁴

These microfluidic systems provide substantial advantages. One of the advantages is the reduction of waste and associated costs due to reduced reagent and sample consumption. Furthermore, high surface to volume ratio and short transport time of samples and reagents in μ TAS allows rapid analysis and high throughput. In addition, the small size and lower power demand increase the portability and automation of μ TAS.^{15,16}

Miniaturisation is more than simply the scaling down of devices, as the relative importance of forces and processes changes with scale. Despite the advantages of μ TAS, there are some challenges to be encountered for *in situ* environmental monitoring such as sample introduction, complexity of the sample matrix, and the low concentration of the analyte of interest in the environment.¹⁷ For instance, due to the low volume capacity in μ TAS, very precise control of sample introduction is needed in order to introduce representative and reproducible samples into the microfluidic chips. Moreover, sample pre-treatment such as filtration and sample pre-concentration must be completed on-chip to allow direct analysis of real samples.¹⁶⁻¹⁸

1.3. Sample introduction in microfluidic system

Sample introduction or injection is defined as ‘the introduction of a reproducible sample into a flowing carrier stream of a manifold without any disturbance to the carrier stream’.¹⁹ Therefore, a reproducible, versatile and precise controllable injection system is crucial in enhancing the performance of μ TAS as it affects the separation efficiency and detection sensitivity. An increased sample volume injected will favour detection sensitivity but on the other hand, it will cause problems such as band broadening.^{20,21} Most of the conventional injectors such as rotary or slide valve injectors are not suitable for a miniaturised environment due to the requirement for very small sample volumes. In general, there are two main injection techniques which are commonly used to introduce samples into a microfluidic device, electrokinetic injection and hydrodynamic injection.

1.3.1 Electrokinetic injection

In electrokinetic injection, samples are introduced into the microfluidic system by applying voltages between the samples and the sample channel on the microfluidic chip. Electrokinetic injection embodies two basic components, electro osmotic (EOF) and electrophoretic (EP) flow which will be further discussed in section 1.3.3. There are two main modes of electrokinetic injection in μ TAS which are the time-based and discrete volume-based.²²

The time-based is also known as gated injection and can be illustrated as the introduction of a sample into the system over a controlled period of time at a known flow rate. This mode offer advantages such as being relatively easy to control and allowing injection of variable sample volume.

On the other hand, the discrete volume-based injection is the introduction of the sample into a channel with a defined volume which acts as the conventional sample loop. Volume-based injection can be further divided into floating or pinched injection modes depending on the application of electric field within the system and the geometry of the

channels. This mode allows reproducible injection of sample and can be easily automated.

In general, electrokinetic injection has several advantages including easy and good control of flow, simplicity to operate and most importantly, it involves no moving parts, just electrodes which are imbedded in the microfluidic device.¹⁹ However, electrokinetic injection suffers from the drawback of electrokinetic biasing of sample in that the injection favour components with a lower electrophoretic mobility. As a result, the sample injected may not be representative of the whole sample.²³

1.3.2 Hydrodynamic injection

Hydrodynamic injection which usually involves mechanical moving parts such as micromechanical pumps, valves and tubing, operates by manipulating the pressure difference between the two channels of the microfluidic device in order to introduce the sample.²³ Even though hydrodynamic injections have some advantages over electrokinetic injection, such as no inherent discrimination in sample injected and no electrokinetic bias present, a well known drawback is the requirement of mechanical moving parts which decreases the portability of the microfluidic chip due to the difficulties in integration of on-chip injector and valves .^{19,24}

1.3.3 Theory of electrokinetic

1.3.3.1 Electro-osmotic flow (EOF)

EOF is the bulk movement of solutions along a channel in the presence of an applied electric field. EOF occurs when an electrical double-layer known as the Helmholtz layer is created at the surface by the electrostatic attraction of cations to the deprotonated silanol groups on the internal glass surface. In the presence of an applied electric field, the outer layer of the double layer is pulled towards the cathode carrying along the bulk solution with it.²⁵

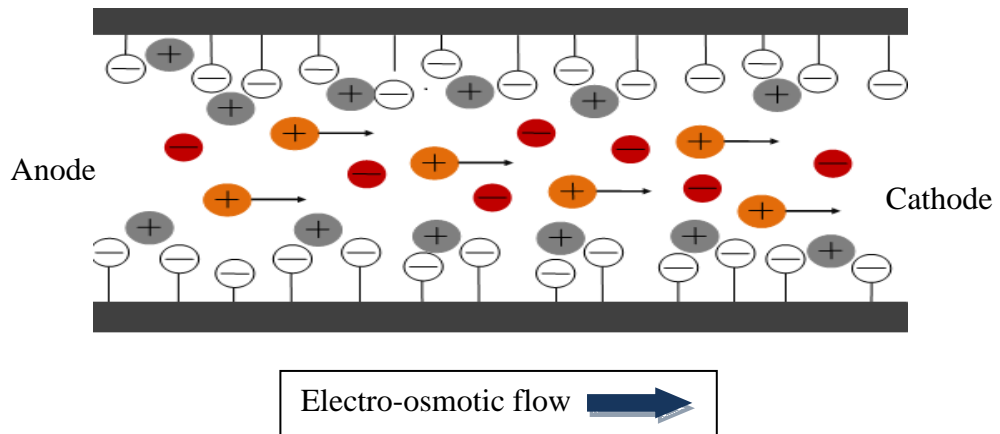


Figure 1.1 Formation of Helmholtz double layer along the walls of a glass microchannel induces electro-osmotic flow towards the cathode.²³

The electro-osmotic mobility (μ_{EOF}) can be described as the bulk fluid velocity through a channel, when an electric field (E) is applied. According to the Smoluchovski equation (Equation 1.1), the magnitude of EOF can be affected by the zeta-potential of the wall (ζ), relative permittivity of medium (ϵ) and the viscosity of the solution (η).²⁶

$$\mu_{\text{EOF}} = -\frac{\epsilon\zeta}{\eta} \quad (\text{Equation 1.1})$$

1.3.3.2 Electrophoretic flow

Electrophoretic flow is the movement of charged particles or ions, relative to a fluid under influence of an electric field. As different species have different effective mobilities, these individual species will migrate at different velocities under constant electric field strength. Therefore, electrophoretic mobility (μ_{EP}) can be defined through a simple relationship shown in Equation 1.2, where μ_{EP} is the constant of proportionality between the migration velocity of a charged species (v) and the electric field strength (E).²⁷

$$\mu_{EP} = \frac{v}{E} \quad (\text{Equation 1.2})$$

Although electrokinetic movement consists of EOF and electrophoretic flow, EOF is usually the dominant force in the movement. This would be a problem for migration of anions as the EOF direction is opposite to the electrophoretic mobilities of anions as shown in Figure 1.2. Therefore, a suppressed or minimal EOF is needed in order for the ions to migrate in their respective directions.²⁸

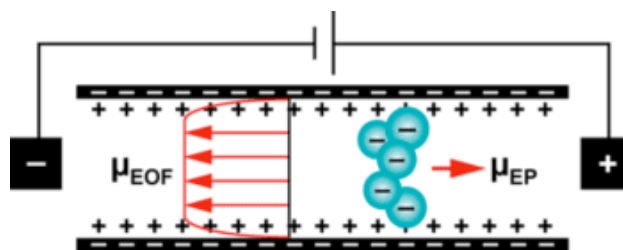


Figure 1.2. EOF in the opposite direction of electrophoretic flow of anions.²⁹

1.4 Sample pre-treatment in microfluidic system

In order to increase portability while allowing autonomous and continuous *in situ* monitoring, the microscale analytical system must have the ability to deal with real samples which can be achieved through sample pre-treatment. Sample pre-treatment is an essential step in analytical chemistry, whereby the sample undergoes some treatments which may involve filtration, extraction or sample pre-concentration before the analysis stage.³⁰

However, to date, many of the sample pre-treatment procedures are still performed manually and off-chip. Such practice, which requires extra time and labour, greatly contradicts the LOC advantage of high portability and automation. Therefore, there have been significant efforts in integration of sample pre-treatment on-chip in the past few years.¹⁸

As the sample pre-treatment procedures have always had to be individually tailored to the type and nature of samples, the following discussion will focus on sample pre-treatment of river water samples. Generally, on-chip sample pre-treatment of water sample can be divided into two main categories^{30,31} :-

- i) The extraction/ clean-up of the analyte of interest from the sample matrix;
- ii) Sample pre-concentration.

1.4.1 Extraction or clean-up of analyte of interest from sample matrix

As the miniaturised μ TAS is characterised by the small dimensions of the microstructure channel network, clogging of channels due to particulate contamination is a common problem. For example, a river water sample consists of particulate and colloids which must be removed prior to analysis, to prevent blockage and disruption of the system.³² The simplest solution is to filter all the reagents and sample prior to introduction. However, most conventional filtration methods such as syringe filters require fluidic volumes much greater than those required for on-chip analytical processing. In addition, filtering is incompatible with the ultimate goal of μ TAS, which is autonomous operation, as most of the conventional methods are manually operated.³⁰ Therefore, it is desirable to integrate a sample-filtration system on-chip prior to analysis. There are two on-chip sample filtration approaches that have been employed: structurally-based filters and diffusion-based filters.¹⁸

Structurally-based filters which involve microfabricated frits, pillar structures or flow restrictors within fluidic channels operate by mimicking the conventional filters. Particulates having a cross-section larger than the featured dimensions of the microstructure are retained behind whilst allowing the passage of smaller analytes.³³ Such designs of microstructure have typically been deployed as bead traps or stationary phase reactors.³¹ An example of a structurally-based filter was suggested by He *et al.* where *in situ* solvent and reagent filters based on the concept of lateral percolation were micromachined into a microfluidic system. The authors successfully restricted particulates with dimensions larger than 1.5 μm without clogging the filters. On top of that, the efficacy of these filters was also examined by filtering solvent containing a variety of particulate materials including dust and bacterial cells.³³

As the microfluidic system has small channel dimension, the dominance of laminar flow normally occurs due to the very low Reynolds number. Under laminar flow, mass transport can only take place via molecular diffusion, and not by turbulence mixing.³⁴ Therefore, filtration through diffusion-based filters can be achieved by allowing two separate laminar flowing sample and solvent streams to be in contact for a certain period of time. Consequently, the analytes of interest which usually have higher mobility

migrate across the laminar boundary between both streams into the solvent stream whilst leaving the unwanted heavier particulates in the original fluid stream.^{31,34}

Brody *et al.* successfully fabricated a diffusion-based filter device, the H-filter which is named after the H-shaped microchannel system (Figure 1.3).³⁴ The H-filter operates by bringing two separate laminar flows from the carrier and diluant streams in contact in the central channel, which allow molecular diffusion to occur. Consequently, only particles in the carrier stream which successfully crossed the fluid barrier into the diluant stream before reaching the exit of the central channel, where both streams are separated, will end up in the filtered output.

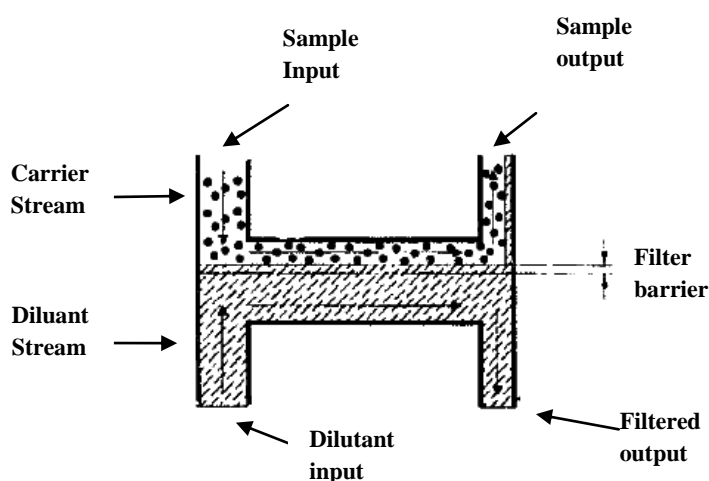


Figure 1.3 The design of H-filter where both streams are in contact in the central channel. Adapted from Brody *et al.*³⁴

Structurally-based filters suffer from the drawback that the efficacy of the filter structure is limited by the resolution limit of the manufacturing process, which would be a problem in filtering sub-micron sized particulates.³¹ Although this is an advantage for diffusion-based filters, as its operation is dependent on the molecular diffusion rather than the resolution of the manufacturing process, the microfabrication process of these filters is very time consuming and requires a very sophisticated technology.¹⁸

1.4.2. Sample pre-concentration

In a miniaturised system, the samples involved are in ultra-small volumes (pL – nL) which contribute to the advantages of fast analysis, low cost and low wastage. However, as a consequence of the low volumes involved, the analyte of interest is often present at very low concentration, which requires highly sensitive detection methods. This is due to the difficulty in detecting signals of low analyte concentrations over the background noise.¹⁶ Although many detection methods have been successfully applied in microfluidic systems, most of these methods have insufficient sensitivity and detection limits. Fluorescence detection, on the other hand, although one of the most sensitive detection methods, is not suitable for application in water analysis as most of the analytes of interest are not intrinsically fluorescent.

Therefore, it is desirable to incorporate sample pre-concentration prior to analysis within microfluidic systems to counteract lower detection sensitivity. Over the last decade, many on-line sample pre-concentration techniques have been developed by a number of researchers. Three of the most widely used pre-concentration techniques are field amplified sample stacking (FASS), isotachopheresis (ITP) and solid phase extraction (SPE).¹⁵

1.4.2.1 Field amplified sample stacking (FASS)

In FASS, a plug of samples in low conductivity buffer is injected into the channel filled with a background buffer which has the same composition but higher conductivity. When a voltage is applied, the electric field strength in the sample zone is higher than in the buffer zone due to conductivity effect, resulting in increased analyte velocity in the sample zone. Pre-concentration is achieved when the analytes decelerate and stack into a narrow sample band at the buffer interface.¹⁵ Although the stacking process of FASS is rapid and efficient for samples in a low conductivity buffer, it suffers from a drawback in dealing with samples containing a high concentration of salts, which may greatly reduce the stacking effect. This is because in samples with high conductivity, it provides a smaller difference in the electric field at the buffer interface.³⁵ As most real

samples contain high concentrations of salts, the applicability of FASS is restricted as it requires some complex sample preparation steps before the stacking process.^{15,16}

1.4.2.2 Isotachopheresis (ITP)

ITP extends the stacking concept of FASS to ternary buffer systems which allow it to be used for both sample pre-concentration and analytical separation purposes. In ITP, a volume of sample is introduced between a leading electrolyte (LE) and a terminating electrolyte (TE). The LE is composed of ions with higher mobility than the sample ions and the TE, while the TE contains ions with lower mobility than any ions in the sample.³⁶ If the system is set up for anionic species, the reservoir containing the LE will contain the anode and the TE reservoir will contain the cathode.³⁷ When an electric field is applied, the mixture of ions will separate from one another forming discrete zones located in between LE and TE in order of descending mobilities as shown in Figure 1.4.

As all the constituents of the sample migrate with the same velocity, which is determined by the velocity of the leading ions, the electric field strength is self-adjusted to maintain a constant velocity in the discontinuous electrolyte system, since the effective mobilities of various ionic species in the system vary (Equation 1.3).^{16,36} This means that the ions with higher mobility will be hindered by the weaker field around them while the ions with lower mobility will be accelerated by the stronger field around them. As a consequence, this self-sharpening phenomenon maintains very sharp boundaries between the zones which lead to separation of different analytes.

$$\text{Velocity} = E (\text{electric field strength}) \times M_{\text{eff}} (\text{effective mobility of species})$$

Equation 1.3

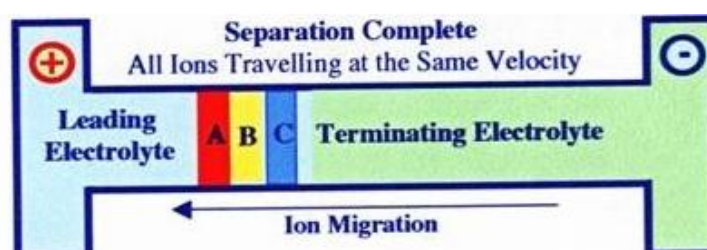


Figure 1.4 Formation of discrete zones of three anions mixture located between LE and TE. All ions travel at the same velocity as the velocity of LE.³⁷

One important characteristic of ITP is that the concentrations of substances in each zone are adjusted to the concentration of the LE according to the Kohlrausch regulating function (KRF). This means that sample zones which are less concentrated than LE will be sharpened into narrower zones, whereas more concentrated zones will be diluted to match up with the concentration of LE. Therefore, pre-concentration or dilution of samples can be tailored by manipulating the concentration of LE.^{30,36}

ITP has been successfully transferred into microfluidic chips and widely applied by a number of researchers for both pre-concentration and separation purposes.^{32,38-43} Chen *et al.* compiled a review discussing the recent developments of ITP in microfluidic chips including its application in analysis and sample pre-treatment of ionic compounds and biomolecules.⁴⁴ For example, Bodor *et al.* demonstrated the separation of inorganic anions present in water samples, using ITP-capillary zone electrophoresis (CZE) coupled separation columns on a microfluidic chip.³² In the ITP stage, the microconstituent analytes (nitrite, fluoride, and phosphate) were concentrated within 3-4 min. As a result, separation and detection of these typical anionic microconstituents in water samples were achieved by CZE with a LOD of 5-7 μM .³²

Although ITP suffers a drawback from its complex buffer system, ITP is one of the most effective on-chip pre-concentration techniques, that provide high concentration enhancement and increased loading capacity.^{16,35} This is important for this project as most of the analytes of interest in river water are present at very low concentration, which in turn causes difficulty in detection using a conductometric detector.

1.4.2.3 Solid phase extraction (SPE)

SPE is one of the useful techniques for sample clean-up and pre-concentration. In SPE, the analyte of interest is retained by chromatographic stationary phase materials and subsequently eluted in an appropriate solvent. Whilst the analyte is retained within the stationary phase, the unwanted components of the sample matrix are eliminated to the waste. As a consequence, sample clean-up and enrichment occur simultaneously.^{31,45} As the capacity of SPE is dependent on the surface area available for interaction, there are three approaches that have been carried out to fabricate SPE stationary phase with different capacities in microfluidic systems: open-tubular SPE, packed-column SPE and monolithic SPE.

Open-tubular SPE involves coating the channel walls with a high affinity stationary phase which will interact with the target analyte. Although this method is relatively simple and does not require any extra stationary phase materials, the capacity of the stationary phase is low as the surface area available for binding in open-tubular SPE is limited.⁴⁵

Packed-column SPE is fabricated by filling or packing the microchannels with a microparticle stationary phase material such as silica beads. This method significantly increases the surface area and loading capacity of SPE. However, packing and retaining these stationary phase materials at specific locations within microfluidic chip may be laborious, time consuming and require undesirable fabrication of frits or weirs.^{31,46}

Monolithic SPE normally involves *in situ* polymerised monoliths as the stationary phase. This continuous, porous monolithic phase has high surface area and simple fabrication procedure where the low-viscosity monomer solution can be introduced into microchannels before initiation by using vacuum or pressure. In addition, as the monolith is attached to the channel walls, there is no need for the fabrication of frits or weirs to retain the stationary phase.⁴⁷ Besides, as the stationary phase for SPE, a monolithic stationary phase has been widely used to perform chromatographic separation, which will be further discussed in section 1.7.

1.5 Separation techniques in microfluidic system for water monitoring

Research has been carried out into miniaturising an *in situ* water quality monitoring system due to the advantages of low reagent consumption, rapid and better analysis, ease of automation, relatively low cost and applicability to *in situ* on field analysis.⁴⁸ Beaton *et al.* have developed an automated LOC colourimetric sensor which integrated the Griess assay for detection of nitrite in seawater. The micro device was successfully operated *in situ* for 57 h continuously and 375 measurements were taken. It is capable of sampling at high frequency and has a low limit of detection of 15 nM.¹¹ Cleary *et al.* have fabricated an autonomous microfluidic-based analyser for determination of phosphate in wastewater. The analyser incorporates a microfluidic chip, colorimetric detection, electronic board and GSM modem into a portable device. The phosphate analyser was successfully used to analyse the wastewater at a municipal wastewater treatment plant and the performance was reported to be comparable with an existing commercially available phosphate analyser.⁴⁹

Most of these successful miniaturised analysis systems developed are selective where only certain nutrients can be analysed at once. However, they are not suitable for this work, which required simultaneous detection of inorganic cations which consists of Na^+ , K^+ , Ca^{2+} , Mg^{2+} , NH_4^+ , and anions consisting of Cl^- , NO_2^- , NO_3^- , PO_4^{3-} , SO_4^{3-} in river water.

The first success in simultaneous analysis of anions through a miniaturised ion chromatography was demonstrated by Murrphy *et al.* They reported a separation of iodide, nitrate, nitrite and thiourea through an anion exchange microseparation column which was coated with quaternary ammonium latex particles although the injection and detection system were off-chip.⁴⁸ Further improvement on miniaturised IC was demonstrated by Kang *et al.* where a conductivity detector was successfully integrated into the system and separation of three anions, chloride, bromide and sulphate, was achieved.⁵⁰ These examples found in the literature suggested the possibility of miniaturising IC for simultaneous ion analysis.

1.6 Background of ion chromatography

The basic theory behind Ion Chromatography (IC) is a combination of chromatography and ion exchange. Adam and Holmes were the first to report the possibility of ion exchange with synthetic ion exchangers by forming cross-linked and insoluble polymers.⁵¹ Many developments have been achieved since, and one of the most remarkable achievements was in 1975, when Small *et al.* introduced a novel ion exchange chromatographic method using conductimetric detection.⁵² With the invention of a “stripper” column or suppressor column, they successfully separated many anionic and cationic species using conductimetric detection and this solved the problem of the need for a good universal detector. During the American Chemical Society convention in Chicago in 1975, Dionex Corporation displayed the first Ion Chromatography instrument containing a suppressor column and this established the new market for IC.

1.6.1. Ion chromatography system

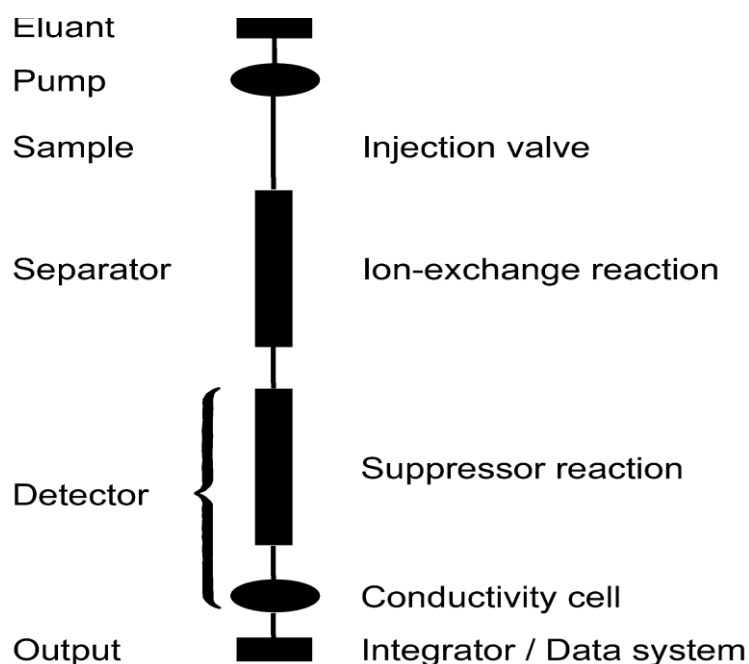


Figure 1.5 Schematic diagram of basic components of an ion chromatograph.⁵³

Generally, a conventional IC operates by the eluent carrying the sample which is injected via sample injection, and flows through the separation column where separation takes place before detection by the flow-through detector. The choice of a suitable detection method depends on the eluents and separation methods used. The conductivity detector is a universal detection system, which is the most common detector applied in IC. This is due to its simplicity and robustness, but more importantly because all inorganic ions are electrically conducting.⁵⁴ Besides the conductivity detector, there are other selective detectors used in IC, such as UV/Vis and fluorescence.

As shown in Figure 1.5, each component in IC plays an important role, especially the separator column, which is the stationary phase that determines the separation mechanism of the whole chromatography. For instance, it decides the type and composition of mobile phase and type of detection system. Ion-exchangers can be classified into two categories: cation-exchange which usually uses the sulfonate group and anion-exchange which is functionalised with the quaternary ammonium group.^{55,56}

The separation in IC is based on the ion exchange principle where the stationary phase provides an ion exchange surface for the analyte ions and counter-ions from the eluent to exchange upon. As different ions have different affinities for the stationary phase, their retention times on the column will vary, which leads to separation.⁵⁵



Equation 1.4 shows an example of the reaction which occurs during ion exchange process on an anion-exchange stationary phase. M^+ denotes the insoluble matrix containing a fixed positive charge; E^- is the counter-ion while A^- is the sample anion. When the eluent containing sample anions, A^- is introduced into the stationary phase, the anions will replace the counter-ion, E^- and be temporarily retained by the fixed positive charge.⁵⁵

The eluent plays a vital role in the separation and elution of analyte ions as it competes with the analyte ions for the fixed charge on the stationary phase. This causes retention and elution of the analyte ions from the stationary phase to achieve the desired separation. There are several characteristics which are important in choosing an eluent,

such as the compatibility with detection system, the nature and concentration of competing ions in the eluent, pH and the buffering capacity of the eluent. Hence, it is important to have a suitable eluent as it manipulates the retention of the analytes, which greatly affects the quality of separation.^{55,56}

The suppression column operates by chemically reducing the background conductivity of the eluting mobile phase before it enters the conductivity detector. This is because conductivity detection gives excellent sensitivity when the conductance of the analyte ion is measured in an eluent of low background conductivity. It can be illustrated through an example of suppression reaction in anion exchange chromatography shown in Equation 1.5.^{55,56}



Equation 1.5 shows that the highly conductive sodium bicarbonate, which is used as the eluent for the separation in anion exchange chromatography is converted into low conductive carbonic acid by exchanging the sodium ions with the protons of the suppressor.⁵⁶

1.6.2. Common applications of IC in water analysis

IC has been widely used for the analysis of water due to its high sensitivity, low limit of detection, stability and the ability of simultaneous determination.⁵⁷ For example, Neal *et al.* reported the simultaneous determination of bromide, chloride, fluoride, nitrate, and sulphate in rainfall, cloud water and river waters using IC.⁵⁸ Fernandez *et al.* demonstrated simultaneous determination of inorganic anions alongside with calcium and magnesium by suppressed IC.⁵⁷ Many regulatory and standards organisations such as ISO and the US Environmental Protection Agency (EPA) have approved the analysis of inorganic ions in water using IC. However, as IC is a laboratory-based instrument, the main limitation of IC is the lack of portability, so that the samples have to be transported back to the laboratory for analysis.

1.6.3 Advances in separation process of IC

In recent years, the most significant advance in IC is the development of porous monolithic media as the stationary phase. These monolithic materials have made a major impact due to their unique characteristics of low pressure resistance and highly efficient mass transfer properties. Since then, numerous new approaches in chromatographic separations of ions have been developed by using monolithic media as the stationary phase. These include ultra-fast IC, micro-IC, and the flow gradients and double gradients in IC.⁵⁹

1.7 Monoliths

A monolith is a bimodal porous structure which is typically fabricated through *in situ* polymerisation of monomers. It consists of small pores within an interconnected skeleton for high surface area and surrounded by large through-pores for high permeability.⁶⁰ Since 1995, when methacrylate monolith was first used successfully as the stationary phase in IC, many research efforts have been made to enhance the efficiency of monolithic stationary phases for chromatographic analysis.⁶¹ Today, monolithic stationary phases are widely used as the separation column for IC due to several advantages^{62,63}:-

- i) High mechanical stability.
- ii) High efficient mass transfer.
- iii) High permeability.
- iv) High surface area.
- v) Low back pressure.
- vi) Simple and *in situ* preparation within a variety of housings.
- vii) Easily modified.

Furthermore, monolithic columns have advantages over packed bed columns, as no frits are required to hold the monolith in place and the monolith has higher tolerance to operate at high flow rate. In addition, due to the large surface area, which leads to higher ion-exchange capacities, monolithic columns are free from drawbacks such as being easily overloaded, a problem suffered by open tubular columns.⁶⁴

Monolithic columns are divided into two categories based on their materials, which are silica and organic polymers. Both silica and organic polymer monolithic columns have been demonstrated as useful stationary phases for IC. Organic polymer monoliths have several advantages such as their high resistance to pH, which allows the usage of strong eluents. A further significant advantage of organic polymer monoliths is their ease of *in situ* preparation in a range of formats.⁶⁵

Although silica-based monolithic columns suffer from the drawback of pH limitation, they offer some advantages over organic polymers such as higher chromatographic efficiency, no swelling or shrinking issues when in contact with organic solvent, along with the availability of a variety of facile post-modification steps available due to high content of silanol groups on the silica surface.^{65,66} Therefore, silica monoliths are better suited for the separation of small analytes of interest in this project due to their high chromatographic efficiency and high surface area.

The sol-gel process, which was first reported by Nakanishi *et al.*, is the most common approach for fabrication of silica monoliths. This is because the silica monoliths fabricated through sol-gel method possess uniform porous morphology with an array of well-ordered interlinked skeleton branches as shown in Figure 1.6.⁶⁷

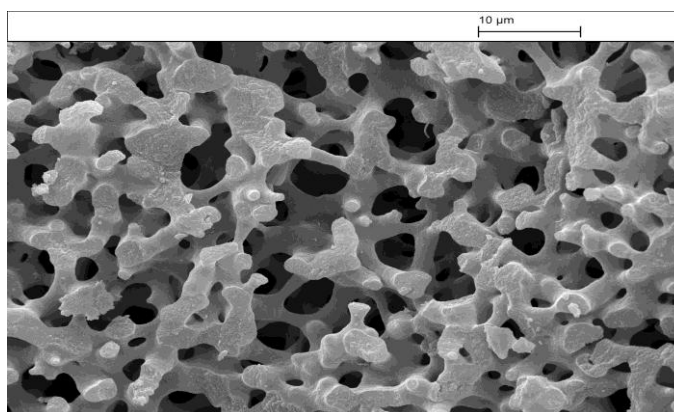


Figure 1.6 SEM image of a silica monolith fabricated through sol-gel method.

As mentioned earlier, many post-modifications on silica monoliths such as surfactant-coating and covalent attachment of functional group substrates have been reported to produce functionalised ion-exchange silica monoliths for rapid and efficient separation. In the early work, Hatsis *et al.* successfully obtained rapid separations of eight inorganic anions within 15 s utilising a reversed-phase (RP) silica monolith with ion-interaction reagent tetrabutylammonium-phthalate.⁶⁸ In later work by the same authors, a RP silica monolith was semi-permanently coated with didodecylmethylammonium bromide (DDAB) surfactant and seven inorganic anions were successfully separated within 30 s using flow rates up to 10 mL/min.⁶⁹

A further example of surfactant coating was demonstrated by Connolly *et al.* who successfully produced both anion and cation exchange silica monolithic columns. The RP silica columns were coated with DDAB to fabricate an anion-exchange column, and with dioctylsulphosuccinate (DOSS) for a cation-exchange column. Rapid separation of eight anions and five cations was achieved within 100 s using indirect conductivity detection when the columns were used individually. The authors also demonstrated the possibility of simultaneous analysis of both anions and cations in water samples by connecting both columns in parallel.⁷⁰ This inspired Victory *et al.* to investigate the potential of μ IC in using ultrashort DDAB-coated silica monolith columns with a combination of micro-scale peristaltic pump for anion analysis.⁷¹

However, Sugrue *et al.* have suggested several drawbacks of surfactant coating such as necessitating a frequent recoating of the column, which is time consuming and will eventually lead to pressure build-ups and poor reproducibility. Therefore, the authors have demonstrated an alternative approach where the ion-exchange groups are covalently attached onto the silica surface. Iminodiacetic acid (IDA), which is a chelating ion exchanger, was covalently bonded on a bare silica monolithic column and rapid separation of alkaline earth metal ions was successfully achieved.⁷²

In addition, Sugrue *et al.* also fabricated a novel zwitterionic ion exchanger silica monolithic column by covalent modification with lysine. The modified column was reported to contain both cation and anion exchange capacity though the capacity for cation exchange was found to be relatively low. The anion exchange capacity was also found to be dependent on the pH of the eluent which can be used to manipulate the

retention of strongly retained anions. Rapid separation of six anions was achieved using the modified column within 100 s with peak efficiencies approximately 50,000 plates/m and variation in retention time % RSD of under 0.3%, indicating sharp and reproducible separation.⁷³

Even though many successes in functionalisation of silica monolith in producing ion-exchange stationary phase have been reported, most of the studies were carried out using commercially available silica monolithic columns which are expensive. An alternative approach to reduce the cost is to self fabricate the silica monolithic column via the sol-gel process based on the hydrolytic polycondensation of alkoxysilanes.^{67,74-77} Huang *et al.* demonstrated functionalisation of lysine on a sol-gel fabricated silica monolith and reported successfully achieved separation.⁷⁶ Furthermore, Lu *et al.* also reported a novel chitosan functionalisation on a self-fabricated silica monolithic column for capillary liquid chromatography.⁷⁷ As cost-effectiveness is one of the areas of consideration in this project, a self-fabricated silica monolithic stationary phase will be a more appropriate approach.

1.8 Aims and Objectives

This environmental research project is an interdisciplinary project involving chemists, engineers and environmental modellers from University of Hull, University of Reading, The Environment Agency (EA), and the Centre for Ecology and Hydrology (CEH).

The main aims of this project for University of Hull are to develop a portable and automated miniaturised total analytical system (μ TAS) that could provide *in situ* chemical measurements over a wide range of nutrients in river water which include cations (Na^+ , K^+ , Ca^{2+} , Mg^{2+} , NH_4^+) and anions (Cl^- , NO_2^- , NO_3^- , SO_4^{2-} , PO_4^{3-})

Therefore, the work reported here forms part of the larger research efforts in the development of a portable and automated miniaturised ion chromatography system for *in situ* high frequency river water monitoring.

The objectives were:

- I. To develop an on-chip sample introduction system which combined electrophoretic injection with sample filtration techniques.
- II. To investigate the possibility of integrating an ITP sample pre-concentration system in a microfluidic chip by encapsulation of all necessary buffers in agarose gel.
- III. To evaluate the possibility of fabrication of an anion exchange column through immobilisation of different ion exchangers for separation purposes using a self-fabricated silica monolithic column.

Chapter 2

**On-Chip Sample Introduction System
with Filtration Mode**

2.1 Introduction

As described in chapter 1, the first objective of this work was to develop an on-chip sample introduction system with sample filtration mode which allows samples to be filtered prior to introduction into the miniaturised system. A river water sample, besides containing the ions of interest, also contains particulates and colloids which are the main factors for channel blockage in a microfluidic chip. Therefore, in the development of an *in situ* monitoring microfluidic system, it is crucial to integrate a filtration system to remove the unwanted particulates while allowing the passage of analytes of interest during sample introduction.

This chapter will report the investigation of combining a potassium silicate frit with electrokinetic injection in a capillary and a microfluidic chip. Electrokinetic injection was selected for use in the system, as it is a well established technique for sample introduction in microfluidic systems and involves no moving parts. As both inorganic cations and anions are of interest in this project, a suppressed EOF injection system is needed for the ions to migrate in their respective directions. An ideal frit for the system should have sufficient mechanical stability to withstand the pressure and adequate flow resistance to prevent bulk flow through the frit. Therefore, a potassium silicate frit was chosen due to its high mechanical stability, simple preparation and reproducibility as suggested by Behnke *et al.*⁷⁸ Due to the small pore size of the fabricated frit, it was used as a filter to prevent unwanted sample matrix and particulates, which are larger than the feature dimensions of the frit entering the system whilst allowing the analyte of interest to migrate through it electrophoretically.³³ In addition, the frits have been reported by Petsul *et al.* to have the ability to reduce hydrostatic flow due to pressure differences that will cause the loss of electrophoretic flow control over the movement of reagents and samples in the system.⁷⁹

2.2. Experimental

As a high voltage was used, a risk assessment was carried out and followed throughout the whole experiment.

2.2.1 Instrumentation

A PCB-mount high voltage (0-2 kV) DC-DC converter power supply (UltraVolt Inc, US) was used to supply high voltage for the electrophoretic introduction of ions through the frit. The conductivity reading was measured using a contactless conductivity detector fabricated in house by a PhD student, Etienne Joly. The concentration of sodium ion was determined using a Corning model 400 flame photometer.

2.2.2 Chemicals and Materials

The frits were prepared using potassium silicate, from VWR International (Leicestershire, UK) and formamide, from Avocado Research Chemicals Ltd (Morecambe, UK). Glycerol, hydroxyethylcellulose (HEC), hydrochloric acid, acetic acid and sodium chloride were obtained from Sigma Aldrich (Dorset, UK). Tris buffer was prepared using tris(hydroxymethyl) aminomethane (Tris), purchased from Fisher Scientific (Leicester, UK). Milli-Q water used for all the experiments was purified by a Milli-Q system from Millipore Ltd (Livingston, UK) with a grade of 18M Ω .cm resistivity.

2.2.3 Fabrication of potassium silicate frit in the capillary and microfluidic chip

A thermally-activated potassium silicate sol-gel monolith was prepared by mixing potassium silicate with formamide in a specific ratio through sonication for 10 min. For the capillary as shown in Figure 2.1, the mixture was then introduced into the capillary (8 cm length with I.D. ~ 0.63 mm) by capillary action until it reached 2 cm length, and then the capillary was rolled horizontally for 15 min before being placed in an oven at 40 °C overnight.⁸⁰ As part of the optimisation study, the influence of experimental parameters such as oven temperature, 40 °C and 100 °C, and incubation time, 6 h and overnight (approximately 16 h) was investigated. In addition, two different ratios of potassium silicate to formamide, 6:1 and 10:1, were used.^{80,81}

For the microfluidic chip as shown in Figure 2.2, a colour dye mixed with glycerol forming a high viscosity coloured mixture was added into the frit chamber before injecting the monolith mixture in order to control the position of the frit. The monolith mixture was slowly pressure injected into the microfluidic chip until it displaced the glycerol in the frit chamber. This was then left in an oven at 40 °C overnight. The remaining coloured glycerol was then removed by washing with Milli-Q water after 2 h in the oven.⁸²



Figure 2.1 The potassium silicate frit made in the capillary.

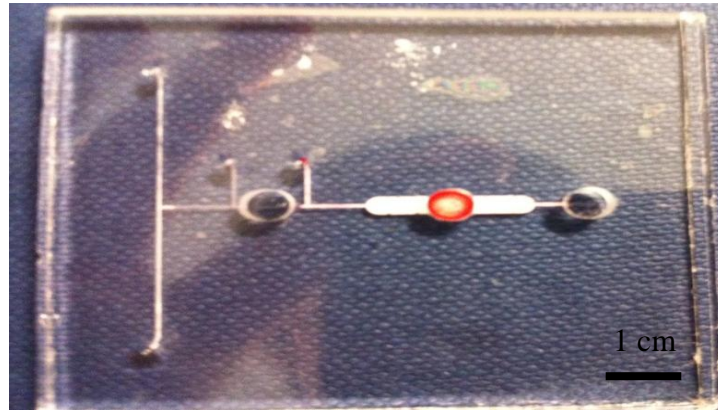


Figure 2.2 The potassium silicate frit made in the microfluidic chip.

2.2.4 Mechanical stability and flow resistance tests for potassium silicate frit in capillary and microfluidic chip

Each frit that was made was tested in two different tests for its mechanical stability and resistance to hydrodynamic and hydrostatic flows, to make sure that it was strong and had adequate flow resistance to prevent liquid migrating through the frit.

In the first test, the frits were tested for mechanical stability and hydrodynamic flow resistance. For capillaries, each of the capillaries with frits installed was connected to a 1 mL disposal syringe by PEEK tubing and Omnifit fittings. Milli-Q water was pumped into the capillary while applying pressure with a flow rate of 0.2 mL/min for 30 s.⁷⁸ For microfluidic chip, the frit was tested by flushing Milli-Q water with a 1 mL disposable syringe which was connected to the opening channel of the chip using epoxy glue while applying pressure at a flow rate of 0.2 mL/min for 30 s. Under applied pressure, the frit was considered mechanically stable if it was not removed from its position and to possess sufficient resistance against hydrodynamic flow provided that liquid failed to be forced through the frit.

In the second test, the “goal post” system as shown in Figure 2.3 was used where the reservoirs at both sides are not filled to the same level, creating hydrostatic flow due to pressure differences.¹⁹ 2 mL of Milli-Q water was filled into reservoir A while reservoir B was filled with 1 mL of Milli-Q water. The heights of water in both reservoirs were

noted. The setup was then sealed and left overnight and the relative heights of the reservoirs were monitored. Similar procedure was applied in the microfluidic chip but with a lower volume of Milli-Q as shown in Figure 2.4. As a result, the frit was considered to have adequate hydrostatic resistance if no movement of liquid was observed in both reservoirs.

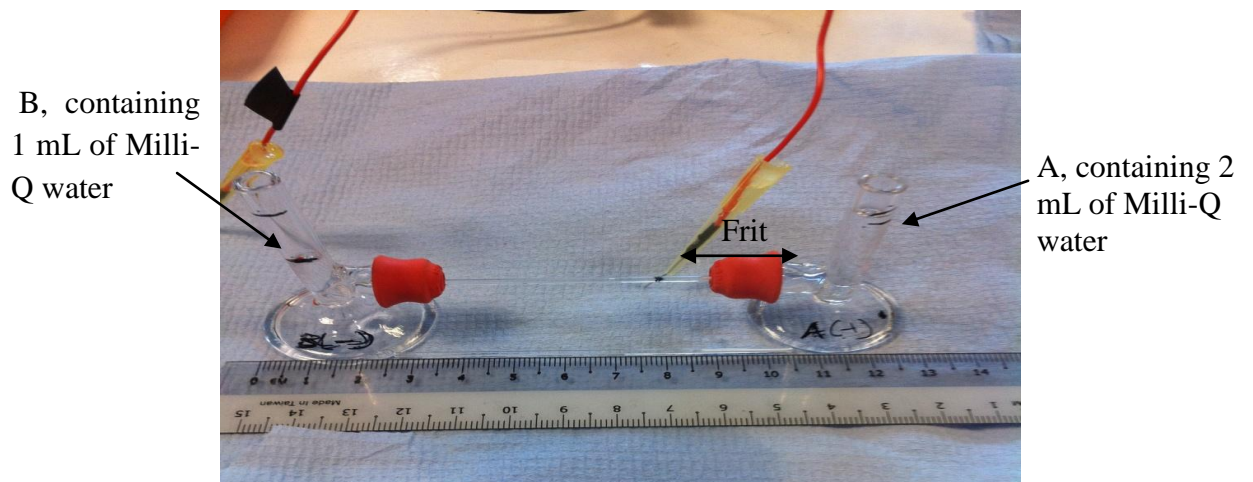


Figure 2.3 The “goal post” system for the hydrodynamic pressure resistance test where reservoir A has higher volume of Milli-Q water than reservoir B.

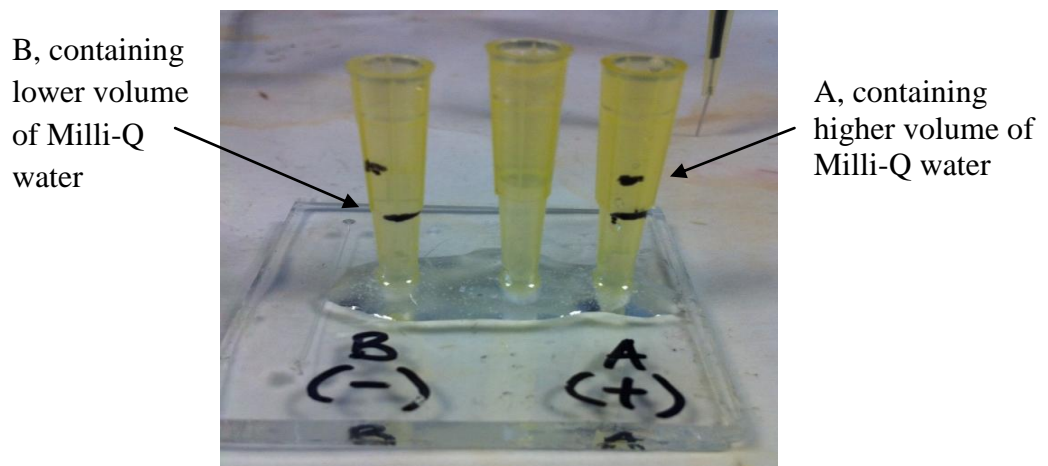


Figure 2.4 The microfluidic chip setup for the hydrodynamic pressure resistance test where reservoir A has higher volume of Milli-Q water than reservoir B.

2.2.5 Preparation of Hydroxyethylcellulose (HEC) solution for EOF suppression

Hydroxyethylcellulose (HEC) solution was prepared by dissolving the HEC powder in tris-acetate buffer pH 8.6 which was prepared from tris(hydroxymethyl) aminomethane (Tris) and acetic acid. The mixture was stirred at 60 rpm for 6 h to fully dissolve the HEC powder. The solution was prepared by this method to prevent the formation of bubbles in the solution and allow uniform mixing.⁸³ A range of HEC concentrations, 0.1%, 0.5%, 1% and 1.5% (w/v) were evaluated for EOF suppression efficiency using the methodology described in section 2.2.6

2.2.6 Investigation of the introduction of ions through the frit in “goal post” system using electrophoretic flow.

The early stage of the investigation was performed, by the “goal post” system as a proof of principle before implementation into the microfluidic chip as the “goal post” system allowed higher volumes of samples to be obtained for analysis, and less effort was needed to fabricate the frit. Due to the limited detector available, sodium ion was chosen as the sample for investigation as it can be easily detected using flame photometry. As this was the preliminary investigation, a high concentration of sodium ions, 10 mM was applied to allow reliable and sensitive measurement of samples.

As shown in Figure 2.5, 2 mL aliquots of sodium sample (10 mM NaCl in 20 mM tris-acetate + HEC) were introduced into the sample reservoir, A, where the anode (+ve) was located, while 2 mL aliquots of 20 mM tris-acetate pH 8.6 + HEC were added to the buffer reservoir, B where the cathode (–ve) was located. Both glass reservoirs were connected by the capillary with the 2 cm frit located at the end of A and the empty section of the capillary was then filled up with similar buffer as in B.

A fixed voltage of 700 V (350 V/cm) was applied for 60 min to allow sufficient time for ion migration.⁸⁰ Throughout the experiment, the current flowing through the “goal post” system was monitored using a voltmeter to make sure that there was not an open circuit

causing system failure. Both samples were then taken to analyse for sodium ions using flame photometer. A series of tris-acetate buffer + HEC with different known concentrations of sodium ions were prepared to provide a calibration curve for each analysis to determine the concentration of sodium ions migrated.

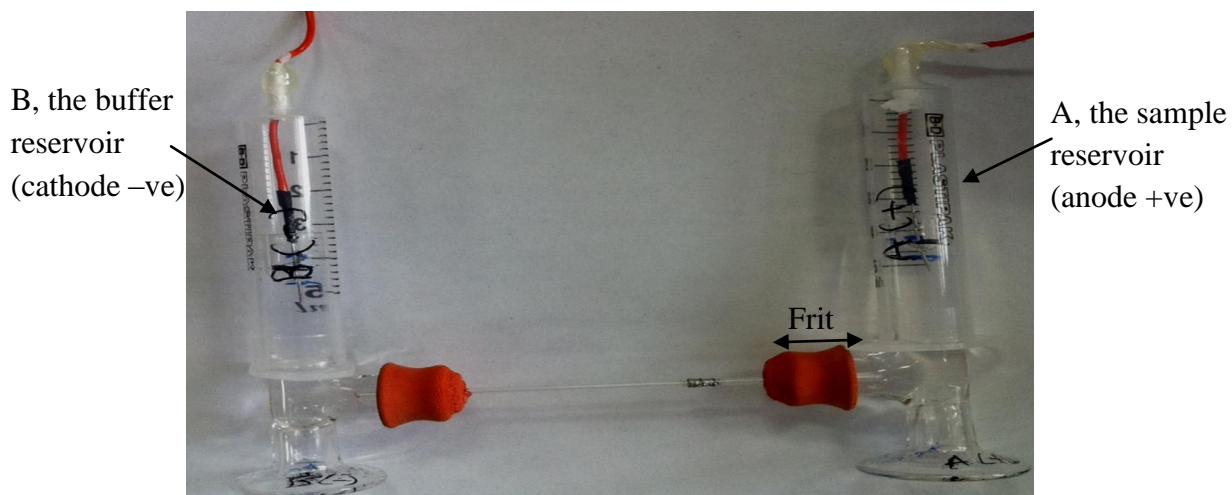


Figure 2.5 The “goal post” setup for the EOF suppressed electrophoretic system.

Investigation was also carried out in collaboration with an Engineering PhD student, Etienne Joly, in utilising a contactless conductivity detector (Figure 2.6) designed and fabricated by him. This preliminary prototype which will be further miniaturised was designed to monitor and record the conductivity changes in the capillary during the migration of ions throughout the investigation.

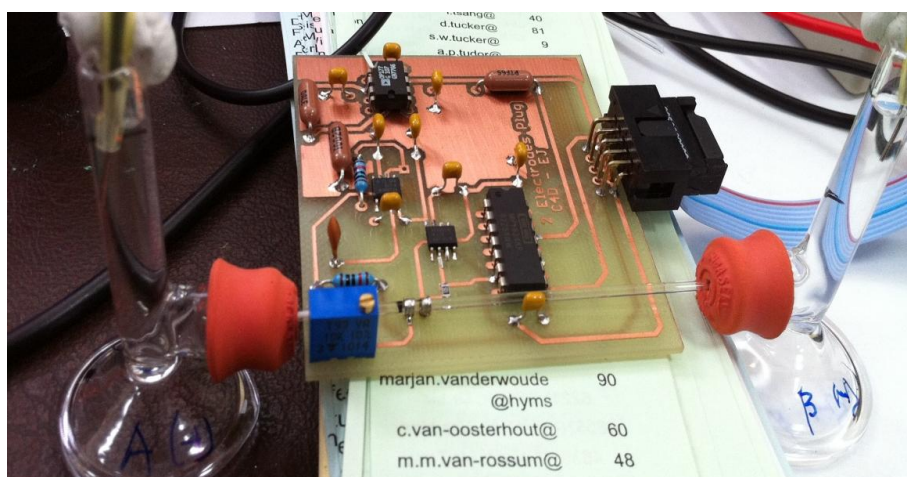


Figure 2.6. Contactless conductivity detector used to monitor the changes of conductivity in the capillary during electrophoresis.

2.2.7 Investigation of ion diffusion through the frit

Ion diffusion investigation was carried out on each frit to determine the amount of ions that diffused through the frit in the “goal post” system and microfluidic chip system without the application of high voltage. The procedure was adapted from the method described by Synder *et al.*⁸⁴ Similar setups shown in Figure 2.3 and Figure 2.4 were used for the investigation.

In both setups, reservoir A was filled with 10 mM NaCl in tris-acetate + HEC while reservoir B was filled with tris-acetate + HEC. Reservoirs A and B in both setups were then sealed to reduce the evaporation effect, and left at room temperature overnight. Samples from both reservoirs were then analysed for detection of sodium ions using a flame photometer.

2.2.8 Investigation of the introduction of ions through the frit in a microfluidic chip using electrophoretic flow

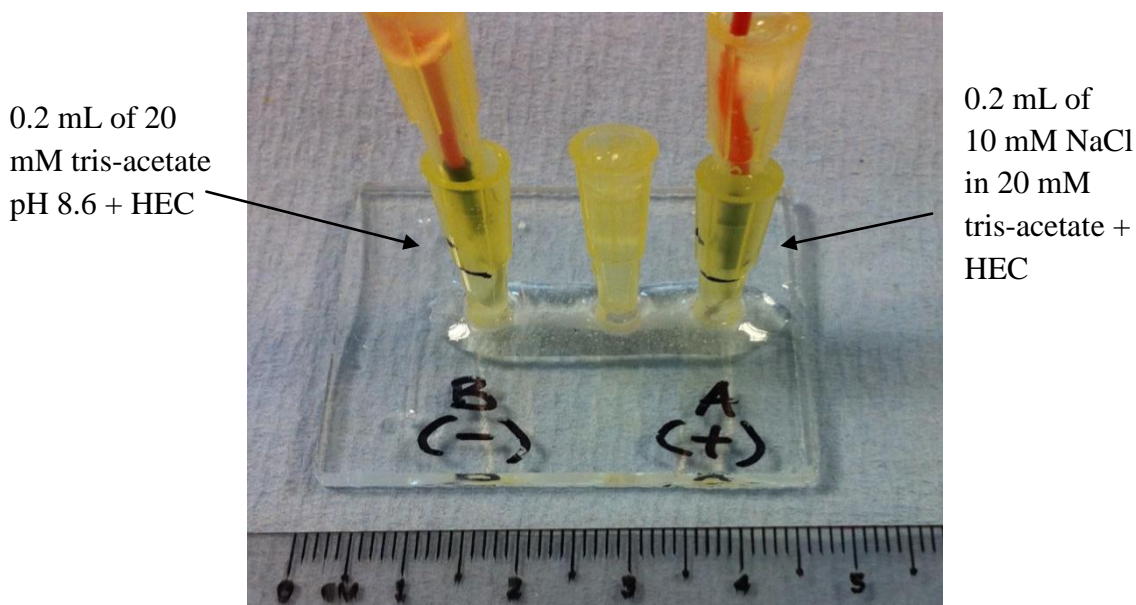


Figure 2.7 The setup for the electrophoretic system in microfluidic chip.

The same procedure as described in section 2.2.6 was applied for the investigation in the microfluidic chip (Figure 2.7). The length of the frit fabricated in the chip was 2 cm which is similar to the length of frit in the capillary. Therefore, a similar voltage of 700 V was applied through the system for 60 min to allow sufficient time for ion migration.⁸⁰ Due to insufficient sample volume needed for analysis, 0.1 mL aliquots of both samples from reservoirs A and B were diluted with tris-acetate + HEC buffer in 1:20 dilution before analysis with a flame photometer. A series of tris-acetate buffer + HEC with different known concentrations of sodium ions were prepared to provide a calibration curve for each analysis to determine the concentration of sodium ions migrated.

2.3 Results and Discussion

2.3.1 Optimisation of experimental parameters for fabrication of frit

As the procedure for fabrication of frit was adapted from Christensen *et al.*⁸⁰, most of the experimental parameters suggested were applied in the investigation. However, optimisation of several parameters such as frit composition ratio, oven temperature and incubation time was necessary due to the smaller porosity size required for filtration purpose. Mechanical stability, hydrodynamic and hydrostatic flow resistance tests as described in section 2.2.4 were carried out as the gauge for the optimisation. The optimisation steps were conducted using the frit in glass capillaries rather than in microfluidic chips due to ease of preparation and lower cost.

2.3.1.1 Frit composition ratio

Table 2.1: The results from the tests of mechanical stability, hydrodynamic and hydrostatic flow resistance on frits fabricated in the capillaries under different frit composition ratios at 40 ° C overnight. (n = 3) Legend: P= Pass F = Fail

Experimental Parameters		Results		
		Mechanical Stability	Hydrodynamic Flow Resistance	Hydrostatic Flow Resistance
Frit composition ratio (potassium silicate : formamide)	10 : 1	P	P	P
	6 : 1	P	P	P

Two different ratios of potassium silicate and formamide, 10:1 and 6:1, as previously reported in literature, were used for the fabrication of potassium silicate frit and the results are summarised in Table 2.1.^{78,80,81} Frits fabricated through both compositions were found to pass all the tests, and hence possessed sufficient mechanical stability and resistance against hydrodynamic and hydrostatic flows.

However, it has been previously reported that formamide is a drying control chemical additive (DCCA) which plays an important role in determining the morphology of the polymeric structure.⁸⁵ The formamide in the potassium silicate solution is hydrolysed into ammonium hydroxide (Equation 2.1) which is the initiator for the polycondensation of silica.⁸⁶ Therefore, increasing the amount of formamide will strengthen the morphology of the frit by increasing the microhardness.⁸⁵



As strong morphology of the frit is required in this project, a 6:1 ratio was used in all subsequent experiments.

2.3.1.2 Oven temperature and incubation time

Previous work by Shaw suggested that decreasing the temperature during the polymerisation process produces frits with smaller pore sizes and higher back pressures which in turn increases the flow resistance.⁸² Therefore, two different oven temperatures were investigated to find out the optimum temperature for the fabrication of frits. Both 40 °C and 100 °C were chosen due to the availability of the oven. In addition, alongside the oven temperature, the incubation times for the polymerisation process were investigated to identify the optimal incubation period. A summary of results obtained from optimisation of oven temperature and incubation time is shown in Table 2.2.

Table 2.2: The results from the tests of mechanical stability, hydrodynamic and hydrostatic flow resistance on frits fabricated in capillaries under different oven temperature and incubation times with frit composition 6:1 (n=3) Legend: P= Pass F= Fail

Experimental Parameters		Results		
		Mechanical stability	Hydrodynamic Flow Resistance	Hydrostatic Flow Resistance
Oven time at 40 °C	6 h	F	F	F
	Overnight	P	P	P
Oven time at 100 °C	6 h	P	F	P
	Overnight	P	F	P

The results in Table 2.2 show that only the frits fabricated at 40 °C overnight passed all the tests. In comparison of frits fabricated at different oven temperatures overnight, all frits were shown to possess high mechanical stability and hydrostatic resistance. However, frits fabricated at 100 °C failed to have sufficient hydrodynamic resistance to prevent liquid from forcing through. It is hypothesised that frits fabricated at 40 °C were fully polymerised forming smaller pore sizes, which in turn increased the hydrodynamic flow resistance. This is in agreement with the results obtained by other workers.⁸²

However, as the results show, the frits left to polymerise at 40 °C for 6 h were very brittle, easily dislodged from their position and had low flow resistance. This might be due to the slow polymerisation rate at 40 °C which requires longer incubation time for the frit to polymerise. An overnight incubation period was proven to allow sufficient time for the polymerisation process to take place in fabricating frits with high mechanical stability and flow resistance.

The overall optimised protocol for fabricating potassium silicate frit can be summarised as below and was used for all the subsequent experiments.

- a) Potassium silicate frit fabricated using a 6:1 ratio of potassium silicate and formamide.
- b) Overnight incubation of potassium silicate frit at 40 °C.

2.3.2 EOF suppression

As mentioned in chapter 1, in electrokinetic injection, the migration of analytes is dependent on two different forces, the electro-osmotic flow and electrophoretic flow. The apparent mobility of the analyte is calculated with the following equation.

$$\mu_{\text{app}} = \mu_{\text{EOF}} + \mu_{\text{EP}} \quad (\text{Equation 2.2})$$

where μ_{app} is the apparent mobility of the analyte, μ_{EOF} is the mobility of electro-osmotic flow, and μ_{EP} is the mobility of electrophoretic flow.

From Equation 2.2, it is obvious that when the electrophoretic mobility of the analyte is low when compared to the EOF mobility, the apparent mobility of the analytes approaches the EOF mobility. For instance, anions with lower electrophoretic mobility than the EOF will be transported according to the EOF direction even though their electrophoretic migration is in the opposite direction. As both cations and anions are of interest in this project, the EOF has to be suppressed to allow migration of ions without being affected by bulk flow (Equation 2.3).

$$\mu_{\text{app}} = \mu_{\text{EP}} + 0_{(\text{EOF suppressed})} \quad (\text{Equation 2.3})$$

Based on the Smoluchowski equation shown in Equation 2.4, the electro-osmotic mobility is influenced by several factors such as the viscosity of the electrolyte and the zeta potential between the bulk solution and fluid-solid interface. Thus, suppression of EOF can be achieved by manipulation of these factors.²⁶

$$\mu_{\text{EOF}} = -\frac{\epsilon\zeta}{\eta} \quad (\text{Equation 2.4})$$

Equation 2.4 shows the Smoluchowski equation where ϵ is the relative permittivity of the medium, ζ is the zeta-potential, and η is the fluid viscosity.

There are two main categories of surface modification on glass capillaries and microfluidic chips for EOF suppression, which are permanent surface modification, and dynamic coating. In permanent surface modification, chemical compounds are bound covalently to the Si-OH groups and alter the surface chemistry. On the other hand, dynamic coating is the adsorption of surface-active compounds on the silica surface.⁸⁷ An overview of the advantages and disadvantages for both categories is stated in Table 2.3.

Table 2.3: An overview comparison of advantages and disadvantages for permanent surface modification and dynamic coating.^{87,88}

Surface Modification Method	Advantages	Disadvantages
Permanent Surface Coating	Stable and do not require regeneration.	Laborious as it requires capillary pre-treatment and introduction of intermediate layer through linking agent.
Dynamic Coating	Easy and simple method, usually by rinsing with coating agent in buffer.	Requires occasional regeneration due to deterioration of performance after repeated runs.

After weighing up the advantages and disadvantages of both methods, dynamic coating was chosen to suppress the EOF due to the ease of preparation and shorter time spent to introduce the coating into the microchannels compared to permanent coating which required a certain level of techniques. In addition, dynamic coating entails no usage of organic solvent, which is harmful if not handled with caution.

Hydroxyethylcellulose (HEC), a widely used cellulose derivative polymer for EOF suppression, was chosen as the coating polymer due to the fact that HEC is nonionic, relatively cheap, and has sufficient hydrophilicity to reduce analyte-capillary surface interaction.⁸⁸⁻⁹⁰ Moreover, HEC was previously reported by Tian *et al.*⁸⁹ to effectively suppress EOF with satisfactory longevity where loss of resolution only occurred after roughly 100 runs of analysis without replenishing the polymer. In addition, Liu *et al.* reported the effective suppression of EOF with HEC over a wide pH range of 3-11.⁹⁰

A range of HEC concentrations, 0.1%, 0.5%, 1% and 1.5% (w/v) were investigated for their EOF suppression efficiency. Whilst increasing the concentration of HEC can further increase the efficiency of EOF suppression, there is a certain concentration threshold where problems in filling up the capillary and microchannel occur due to increased viscosity. The problem was found to be apparent at 1% and 1.5% (w/v) concentrations of HEC where highly viscous solutions were formed. On the other hand, investigation of the EOF suppression efficiency of each of the HEC concentration showed that EOF was successfully suppressed even at 0.1% (w/v). As the viscosity was the lowest with 0.1% (w/v), this concentration was initially chosen for EOF suppression in the “goal post” system. However, the EOF suppression with 0.1% (w/v) of HEC was then found to be inconsistent when applied in the microfluidic chip. Therefore, in order to compromise between the viscosity and EOF suppression efficiency, 0.5% (w/v) of HEC was chosen to be the optimum concentration for EOF suppression in all subsequent investigations in the microfluidic chip.

2.3.3 Selection of buffer

A buffer solution is important in electrophoresis as it will affect the EOF, since a change in pH could alter the zeta potential due to modification of the surface charge of the silica surface.^{26,91} In addition, as sodium ion was chosen as the sample ion in the preliminary investigation due to the limited availability of detector, the buffer had to contain a negligible amount of sodium ions in order to provide minimal background noise. Tris buffer was chosen as the buffer for the investigation as it contained an insignificant amount of sodium ions (refer to Table 2.4) On top of that, tris buffer has previously been used by Tian *et al.* as the buffer for EOF suppression using HEC.⁸⁹

The pH of the buffer was selected to be pH 8.6, which is within the effective pH range of between 7 and 9 due to its pKa value of 8.06 (at 25 °C). In addition, pH 8.6 was previously used in other work as the optimal pH for EOF suppression by HEC and it was shown to increase the longevity of the EOF suppression effect.⁸⁹ Initial pH modification of the buffer was carried out using hydrochloric acid (HCl); however, it was then found that the concentration of chloride in the buffer was too high causing saturation of chloride ions. Although chloride ions were not involved in this preliminary investigation, chloride ions were one of the anions of interest in this project, and the saturation of chloride ions would be a problem in further development of project. Hence, acetic acid which contains a lower amount of chloride was used to replace HCl, forming tris-acetate buffer.

As the buffer concentration alters the ionic strength of the buffer, which affects the zeta potential and EOF, the concentration of the buffer in the preliminary investigation was fixed at 20 mM. The concentration of tris-acetate buffer was chosen as it was previously reported to provide satisfactory stability and repeatability of EOF.²⁶

2.3.4 Electrokinetic injection of sodium ions through frit in capillary in “goal post” system

Initial investigation of introduction of sodium ions through the frit was conducted by an electrokinetically-driven injection system to determine the possibility of introducing ions through the frit by electrokinetic flow, despite having high hydrodynamic flow resistance and back pressure. It is hypothesised that if sodium ions were to successfully migrate through the frit by electrokinetic flow, frit with small pores was fabricated instead of a fully blocked frit. In order to investigate whether this may be the case, the investigation described in section 2.2.6 was carried out in an unsuppressed EOF buffer system. A negative control containing no sodium ions was investigated alongside to determine the amount of sodium ions present in the tris-buffer. The calibration curve and results are summarised in Figure 2.8 and Table 2.4.

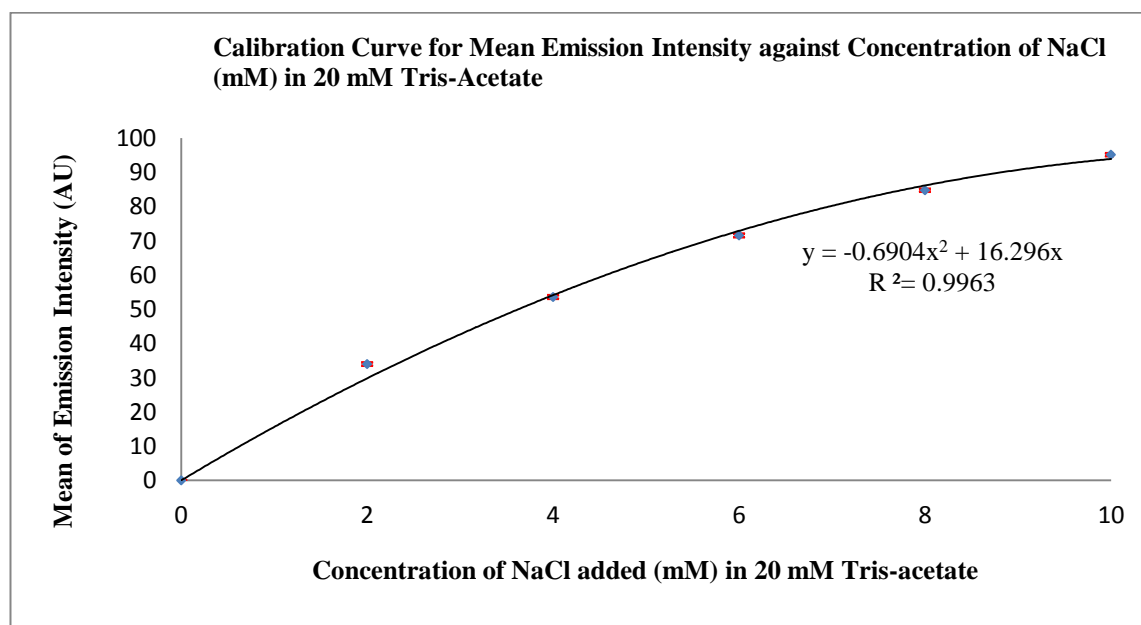


Figure 2.8 The calibration curve for sodium ions with concentration ranging from 0 to 10 mM in 20 mM Tris-acetate pH 8.6 (unsuppressed EOF system), n=10

Table 2.4 The mean of emission intensity and amount of sodium ions migrated under electrokinetic-driven flow at 700 V for 60 min in “goal post” system.

Purpose of Experiment	Sample		Mean of Emission Intensity (n=3)	Concentration of Sodium Ions (mM)
As negative control to investigate the amount of sodium ions in the buffer.	20 mM Tris-acetate (anode)	Before Experiment	0 ± 0	0.00
		After Experiment	0 ± 0	0.00
	20 mM Tris-acetate (cathode)	Before Experiment	0 ± 0	0.00
		After Experiment	0 ± 0	0.00
Evaluate the possibility of introducing sodium ion through the frit by electrokinetic injection.	10 mM NaCl in 20 mM Tris-acetate (anode)	Before Experiment	95.2 ± 0.45	10.00
		After Experiment	83 ± 0	7.44
	Tris- Acetate 20 mM (cathode)	Before Experiment	0 ± 0	0.00
		After Experiment	28.3 ± 0.58	1.88

As can be seen from Table 2.4, it was shown that no sodium ions were present in the tris-acetate buffer. This showed that the background noise in the system was minimal which in turn improved the detection limits in the investigation.

The results from the experiment indicated that sodium ions were successfully migrated through the frit by electrokinetically-driven flow despite having high back pressure and flow resistance. Although the ion migration efficiency was low, 18.8 %, the results proven that the frits fabricated were porous and allowed migration of small ions through them while preventing the passage of large particulates.

However, it was found that the amount of sodium ions recovered from both reservoirs was lower than the initial amount of sodium added. It may be possible that the sodium ions were retained by the potassium silicate frit.

As EOF was not suppressed in this investigation, a slight increase in volume of the reservoir in the cathode was observed indicating the presence of EOF in the system. Further investigation was conducted where the EOF was suppressed to allow only electrophoretic movement of ions, in order to evaluate the possibility and ion migration efficiency through the frit by electrophoretic flow.

Initial suppression of EOF in the “goal post” system was performed by using 0.1% (w/v) HEC in pH 8.6 tris-acetate buffers and the calibration curve and results are recorded in Figure 2.9 and Table 2.5.

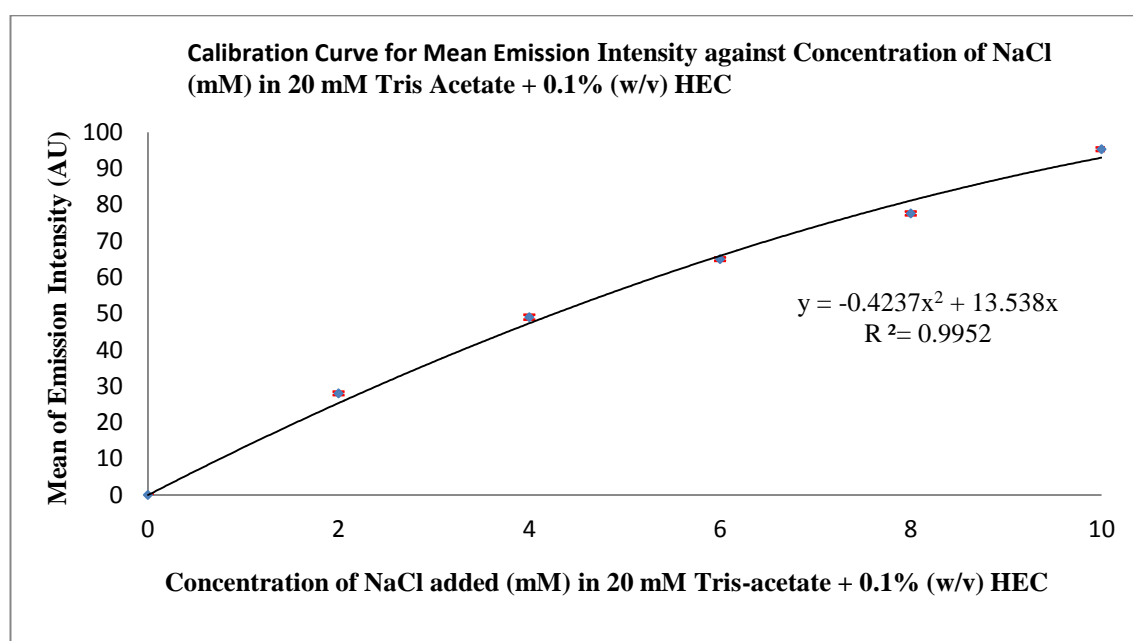


Figure 2.9 The calibration curve for sodium ions with concentration ranging from 0 to 10 mM in 20 mM Tris-acetate pH 8.6 with 0.1% (w/v) of HEC added to suppress the EOF. n=10

Table 2.5 The mean of emission intensity and amount of sodium ions migrated through frit in capillary by electrophoretic flow in “goal post” system at 700 V for 60 min.

Purpose of Experiment	Sample		Mean of Emission Intensity (n=3)	Concentration of Sodium Ions (mM)
To investigate the possibility of introduction of sodium ions through frit by electrophoretic flow.	10 mM NaCl in 20 mM Tris-acetate + 0.1% HEC (anode)	Before Experiment	95.3 ± 0.58	10.00
		After Experiment	84 ± 0	8.42
	Tris- Acetate 20 mM + 0.1% HEC (cathode)	Before Experiment	0 ± 0	0.00
		After Experiment	18 ± 0	1.39

The EOF was shown to be suppressed by using 0.1% (w/v) HEC as no changes of volume in both reservoirs were observed throughout the experiment which indicated no bulk movement of solution. As shown in Table 2.5, the migration of sodium ions through the frit by electrophoretic flow was achieved under the suppression of EOF. However, as expected, the ion migration efficiency (13.9 %) was lower compared to the non EOF-suppressed system, as the ions movement of sodium was driven only by electrophoretic flow.

An investigation of ion diffusion as described in section 2.2.7 was conducted to ensure the migration of sodium ions was not due to diffusion.

Table 2.6 shows the mean emission intensity and amount of sodium ions recovered in both reservoirs after the diffusion test.

Purpose of Experiment	Sample		Mean of Emission Intensity (n=3)	Concentration of Sodium Ions (mM)
To investigate the amount of sodium ions diffused through the frit.	10 mM NaCl in 20 mM Tris- acetate + 0.1% HEC (anode)	Before Experiment	95.3 ± 0.58	10.00
		After Experiment	95.0 ± 0	10.00
	Tris- Acetate 20 mM + 0.1% HEC (cathode)	Before Experiment	0 ± 0	0.00
		After Experiment	0 ± 0	0.00

It was found from the diffusion test that no sodium ions diffused through the frit, as shown in Table 2.6. This confirms that the migration of sodium ions through the potassium silicate frit was due to electrophoretic flow and no other forces.

As the investigation in the “goal post” system was a proof of principle experiment, the results obtained have verified the potential for utilising potassium silicate frit as a filter which allows the migration of small ions through it electrophoretically while having high hydrodynamic and hydrostatic flow resistance.

This work was further expanded into a microfluidic chip in order to ascertain the possibility of miniaturising the sample introduction system and evaluate the potential problems. In order to establish similar electrophoretic mobility in the microfluidic chip, the investigations were designed such that the applied voltage and surface chemistry were the same as the parameters used in the “goal post” system.⁹²

2.3.5 Preparation of potassium silicate frit in a microfluidic chip

Potassium silicate frit was successfully fabricated in the microfluidic chip using the optimised protocol. However, it was found that the precise placement of frit within the frit chamber of microfluidic chip was difficult. Confinement of the frit was achieved by first filling the frit chamber with a highly viscous glycerol solution to which a coloured dye was added. The solution provides resistance to the potassium silicate/formamide solution, before the introduction of the frit mixture. The purpose of adding coloured dye to the glycerol was to increase the visibility of the glycerol, which allowed the position of the glycerol to be monitored when displaced by the frit mixture. The glycerol which was moved into the surrounding channels restricted the movement of the frit mixture, therefore confining it to the frit chamber.

Tests of mechanical stability and flow resistance as described in section 2.2.4 were conducted on the frit fabricated in the microfluidic chip, in order to make sure the frit had the same characteristics as the frit fabricated in the capillary. Positive results were obtained as the frit in the microfluidic chip passed all the tests, thereby confirming that the frit fabricated under the optimised protocol in microfluidic chip had sufficient mechanical stability and resistance against hydrodynamic and hydrostatic flows.

2.3.6 Electrophoretic injection of sodium ions through frit in a microfluidic chip

A microfluidic chip as shown in Figure 2.7 was used to miniaturise the electrophoretic sample introduction system with the frit fabricated within. Initial studies of electrophoretic injection in the microfluidic chip involved suppression of EOF using 0.1 % (w/v) HEC as the concentration has been successfully applied to suppress EOF in the “goal post” system. However, as discussed earlier in section 2.3.2, it was soon found that the suppression of EOF by 0.1 % (w/v) HEC in the microfluidic chip was inconsistent and had poor reproducibility. Therefore, a higher concentration of HEC, 0.5 % (w/v) was selected and the EOF was shown to be successfully suppressed.

To evaluate the possibility of miniaturising the sample introduction system in the microfluidic chip, investigation as described in section 2.2.8 was carried out and the calibration curve and results are summarised in Figure 2.10 and Table 2.7.

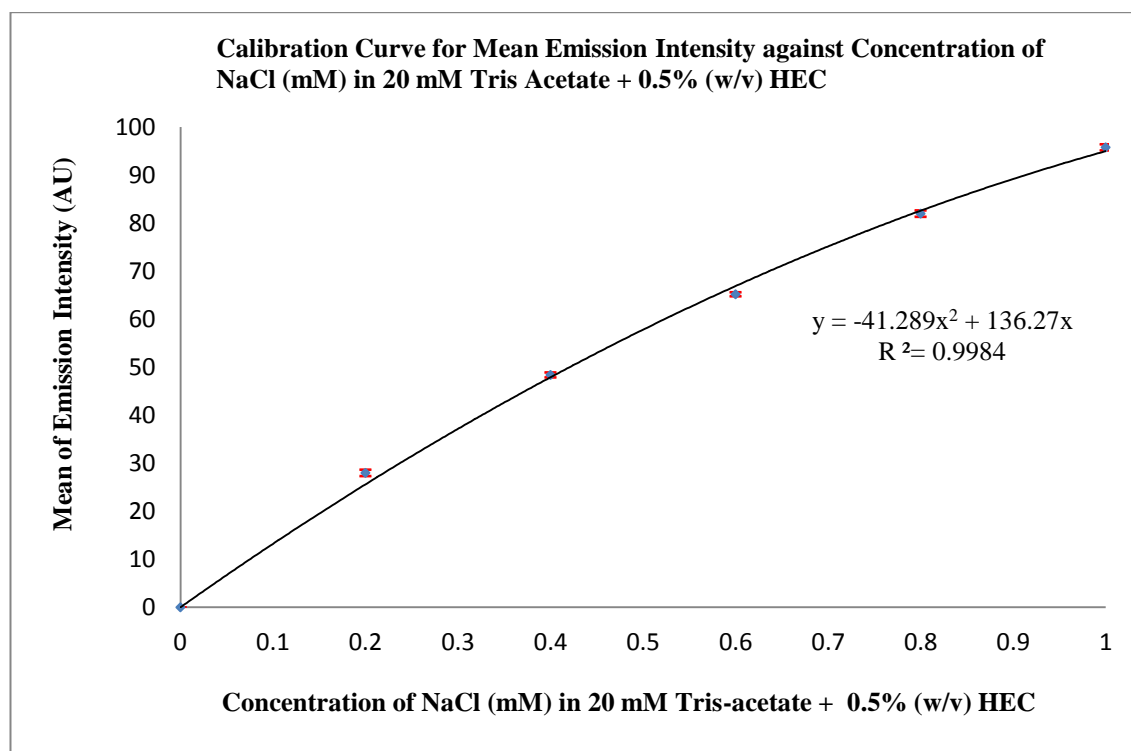


Figure 2.10 The calibration curve for sodium ions with concentration ranging from 0 to 1 mM in 20 mM Tris-acetate pH 8.6 with 0.5% (w/v) of HEC added to suppress the EOF. n=10

Table 2.7 The mean emission intensity and the diluted and original concentration of sodium ions migrated through frit in a microfluidic chip by electrophoretic flow at 700 V for 60 min.

Sample	Contents	Mean Emission Intensity (n=2)	Diluted Concentration of Sodium Ions (mM)	Original Concentration of Sodium Ions (mM)
A	0.1 mL aliquot of sample from anode diluted with 1.9 mL of tris buffer + HEC (1:20 dilution)	42±0	0.34	6.8
B	0.1 mL aliquot of sample from cathode diluted with 1.9 mL of tris buffer + HEC (1:20 dilution)	17±0	0.13	2.6
C	0.1 mL of 10 mM NaCl in 20 mM tris-acetate + 0.5% HEC diluted with 1.9 mL of tris buffer (1:20 dilution)	59±0	0.51	10.2

As can be seen from Table 2.7, samples A and B were the diluted samples prepared after the electrophoretic injection by diluting with 20 mM tris-acetate + 0.5% HEC buffer due to insufficient sample volume available for analysis. Sample C was prepared to determine the initial concentration of sodium ions present in sample A before the electrophoretic injection.

Sodium ions were shown to successfully migrate through the potassium silicate frit by electrophoretic flow with ion migration efficiency of 26%. An ion diffusion test as described in section 2.2.7 was conducted and it was found that no sodium ions were diffused through the frit, thereby further confirming that the ion migration was due to electrophoretic flow. Even though similar electrophoretic mobility was established, the ion migration efficiency obtained in the microfluidic chip was found to be higher compared to the capillary which may be due to more efficient EOF suppression. Despite the higher efficiency obtained, the ion migration efficiency was still low; thus, further optimisation of other factors such as voltage and experimentation time was required.

2.3.7 Development of a contactless conductivity detector

As mentioned in section 2.2.6, a further development of the sample introduction system was carried out in collaboration with an Engineering PhD student, Etienne Joly, in integrating an in-house contactless conductivity detector into the system. As the conductivity reading increases during the migration of ions from the sample into the system, integration of a contactless conductivity detector in the system would allow real-time monitoring of the ion conductivity. This would in turn enable users to constantly monitor the performance of the electrophoretic injection system as well as to detect system failure.

An initial prototype of the contactless conductivity detector (refer to Figure 2.6) was designed to monitor the changes of conductivity in the capillary rather than in the microfluidic chip as it is more easily fabricated, controlled and optimised. Generally, the contactless conductivity detector was installed in a confined area on the outer capillary close to where the frit was located, and it detected the conductivity reading within that specific area. As ions migrated through the area during electrophoretic injection, the contactless conductivity detector detected the conductivity changes.

An initial investigation was carried out by flushing the capillary with a series of standard sodium chloride solutions of different known concentrations ranging from 0 to 1 mM to determine the sensitivity of the detector. A calibration curve was obtained from the investigation and recorded in Figure 2.11.

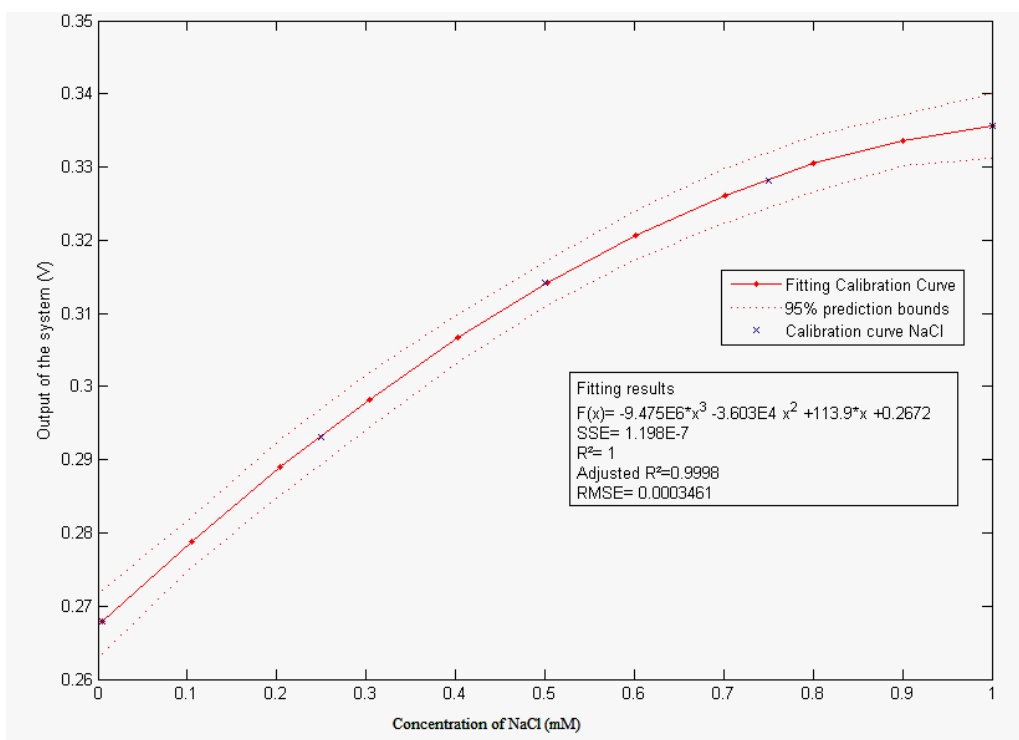


Figure 2.11 The calibration curve for the contactless conductivity detector obtained for sodium ions with concentration from 0 to 1 mM.

As can be seen from Figure 2.11, the contactless conductivity detector was shown to be capable of detecting and distinguishing between different concentrations of sodium flowing through the capillary with sufficient sensitivity in monitoring the conductivity changes.

A further investigation was carried out by implementation of the contactless conductivity detector into the “goal post” system while conducting an electrophoretic introduction of sodium ions through the frit in the capillary. Two attempts were carried out under the same conditions and the conductivity changes during the electrophoretic injection were recorded in Figure 2.12.

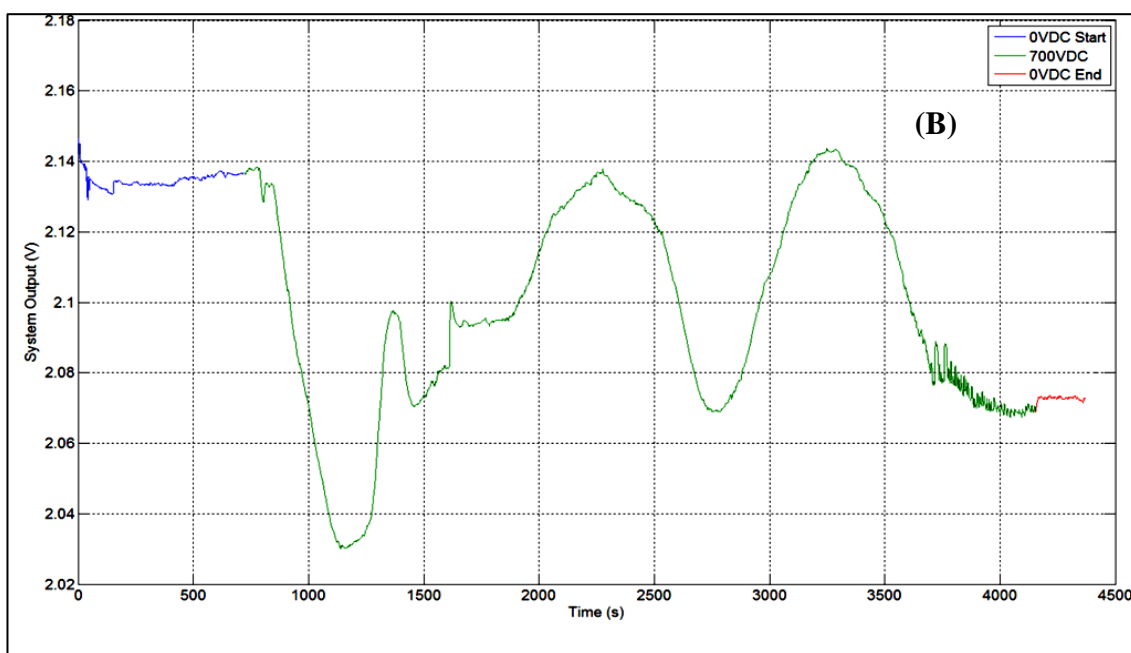
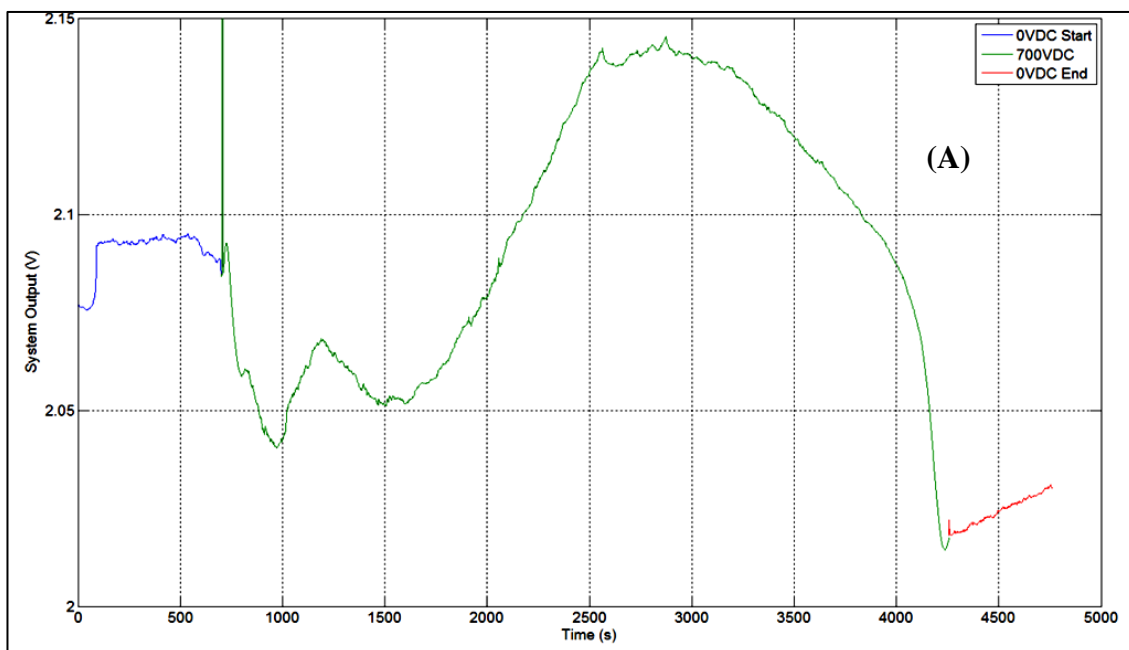


Figure 2.12 The conductivity changes recorded by contactless conductivity detector in two similar attempts of electrophoretic introduction of sodium ions through frit in a capillary in a 20 mM tris-acetate + 0.5% (w/v) HEC buffer system.

Legend: (—) indicates the beginning of experiment when no voltage was supplied, (—) indicates when the voltage was applied, (—) indicates the end of the experiment and no voltage was supplied.

As shown in Figure 2.12, successful detection of conductivity changes within the capillary during the electrophoretic introduction of sodium ions was achieved using the contactless conductivity detector. However, both graphs were found to show sporadic patterns and differed from each other despite similar experiments being conducted. The conductivity readings for both graphs were stable at the beginning of the experiment when no voltage was supplied to cause any migration and movement of ions that would affect the conductivity reading. However, as can be seen from both graphs, the conductivity readings were inconsistent once the voltage was supplied. These sporadic patterns and formation of broad peaks may be due to interference from the potassium silicate frit during the migration of sodium ions. Piraino *et al.* investigated this phenomenon in CEC and explained that peak broadening was attributable to the retention of ions on the surface of the potassium silicate frit during the migration.⁸¹ The conductivity reading dropped when the ions were retained by the frit and increased when the ions were released and migrated through the detection window. A minor baseline drift observable from Figure 2.12A at the end of experiment when the voltage was stopped may be due to the changes in temperature inside the capillary.⁷⁸

As the aim of the sample introduction system is to filter and introduce the sample ions into the system and not for separation, peak broadening was not a major issue, as the performance of the migration of ions could still be monitored based on the conductivity changes. Further development and optimisation were required in order to implement the contactless conductivity detector into a microfluidic chip. As the frit was fabricated for filtration purposes, further work such as silanisation of the frit would be required to reduce the interference.

2.3.8 Conclusion

This chapter has shown the possibility of integrating a sample introduction system coupled with filtration frit in a microfluidic chip. Optimisation of the fabrication of potassium silicate frit was carried out and the frit was successfully proven to possess high mechanical stability and flow resistance against hydrodynamic and hydrostatic flow. In the preliminary study, sodium ions were successfully shown to be capable of being introduced through the frit by electrophoretic flow despite having high flow resistance. Suppression of EOF which allowed migration of ions into the system without the bulk movement of solutions was shown to be achieved by using 0.5% (w/v) HEC. These preliminary results indicated that electrophoretic introduction of ions through filtration frit could be successfully performed in a microfluidic chip, though further optimisation work is required to increase the ion migration efficiency. A contactless conductivity detector was proven to be capable of detecting the conductivity changes during the ion migration, although peak broadening was observed. The integration of the detector could allow real-time monitoring making sure that the ions are migrating properly and efficiently without any disturbances such as bubbles that could retard the migration process and cause system failure.

Chapter 3

Sample Pre-concentration with Miniaturised Isotachophoresis

3.1 Introduction

On-chip sample pre-concentration is crucial in this project as the analytes of interest in river water samples are often present at extremely low concentrations. This causes the detection to be very difficult to achieve, which usually requires highly sensitivity detection techniques such as fluorescence detection. However, this detection technique would not be suitable for river water analysis as most of the analytes of interest are not intrinsically fluorescent. An alternative approach to increase the sensitivity of analyte detection is to pre-concentrate the river water sample prior to analysis. Miniaturised isotachopheresis (ITP) has been widely reported for on-chip sample pre-concentration and separation purposes.^{32,38-43} As the microfluidic system was designed to provide continuous *in situ* monitoring, the sample pre-concentration system had to be automated. However, due to the complexity of the ternary buffer systems in ITP which involved two different electrolytes, introduction of these buffers in a timely and cost-effective manner for *in situ* analysis would be a difficult task. One possible solution is to encapsulate all the required electrolytes buffers in agarose gel and pre-loaded into the microfluidic system. Such encapsulation of reagents in agarose gel has been reported by Oakley *et al.*, who showed that the encapsulated reagents were stable for up to four weeks, when stored at 4 °C.⁹³

Therefore, the aim of the work described in this chapter is to investigate the possibility of integrating an ITP sample pre-concentration system in a microfluidic chip by encapsulation of all necessary buffers in agarose gel. In order to investigate the potential of gel encapsulation, an investigation was conducted based on a simple ITP buffer system reported by Prest *et al.*³⁹ for sodium ions in both a “goal post” system and a microfluidic chip.

3.2 Experimental

As a high voltage was used, a risk assessment was carried out and followed throughout the whole experiment.

3.2.1 Instrumentation

A high voltage power supply unit 1 kV by Kingfield Electronics Ltd was used to supply high voltage for the isotachopheresis. The conductivity and resistance of the agarose gel rod containing both electrolytes were measured using a Wayne Kerr Precision Component Analyser 6430A. The concentration of sodium ion was determined using an ICP-OES Optima 5300DV system.

3.2.2 Chemicals and Materials

The ITP electrolyte buffer system was prepared using hydrochloric acid, hydroxyethylcellulose (HEC), and carnitine-HCL which were all purchased from Sigma Aldrich (Dorset, UK). Agarose powder and the sodium chloride were also obtained from Sigma Aldrich (Dorset, UK). Milli-Q water used for all the experiments was purified by a Milli-Q system from Millipore Ltd (Livingston, UK) with a grade of 18 M Ω .cm resistivity.

3.2.3 Encapsulation of leading electrolyte (LE) and terminating electrolyte (TE) in agarose gel for ITP in “goal post” system

Proof of principle studies were carried out in a “goal post” system rather than microfluidic chip as it was much easier to control and optimise the encapsulation processes. Encapsulation of both LE and TE in agarose gel was prepared in a 6 cm length with 4.3 mm I.D. 1 mL disposable syringe where both ends were cut to have a similar diameter. Both LE and TE were prepared with the procedure suggested by Prest *et al.*³⁹ Agarose powder was added to LE consisting 10 mM HCl and 0.1% (w/v) HEC and TE containing 10 mM carnitine-HCL. The mixture was then heated up to fully dissolve the agarose powder and without stirring as it causes the formation of bubbles. With one end of the syringe sealed with parafilm, the molten mixture of agarose containing LE was added until it half-filled the syringe. This was left to cool vertically for ~5 min, before the mixture of agarose containing TE was added to fill up the syringe. The syringe was then allowed to cool at room temperature ~20 °C for 30 min and stored at 4 °C. A series of agarose gel concentrations, 0.1 %, 0.5 %, 1 % and 2 % (w/v) were investigated to determine the optimum concentration of gel for the encapsulation of electrolytes.

3.2.4 Encapsulation of leading electrolyte (LE) and terminating electrolyte (TE) in agarose gel for ITP in microfluidic chip

The procedure as described in section 3.2.3 was applied for the preparation of both agarose gel mixtures containing the electrolytes. The molten agarose mixture containing LE was introduced into the channel of the microfluidic chip using a 1 mL disposable syringe. The agarose mixture was filled up to half the length of the channel and left to cool before introducing the agarose mixture containing TE to fill up the whole channel. The fully-filled microfluidic chip was allowed to cool under room temperature ~20 °C for 30 min and stored at 4 °C.

3.2.5 Preliminary investigation of ITP using agarose encapsulated electrolytes buffer system in “goal post” system

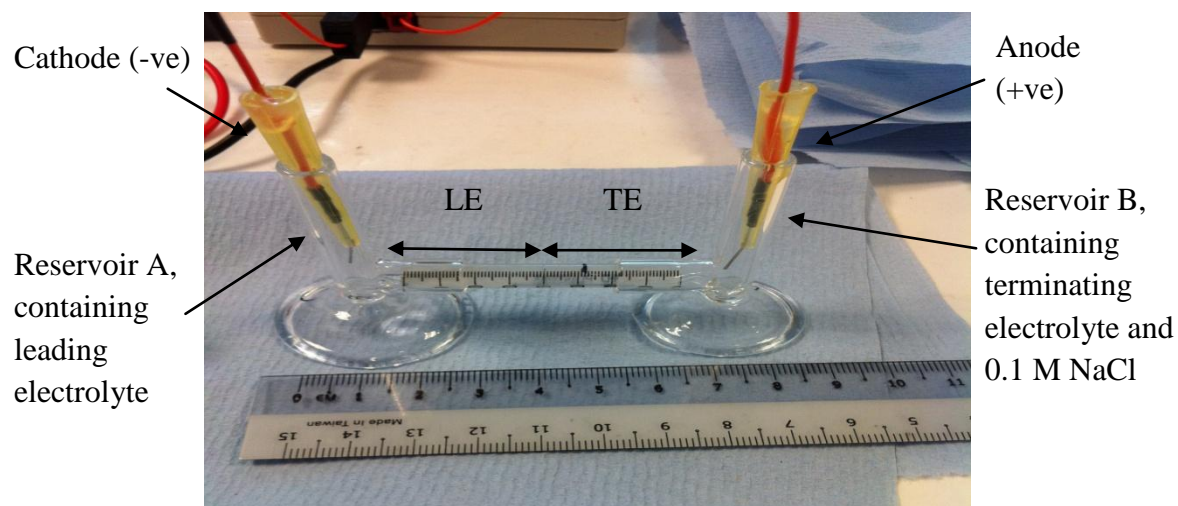


Figure 3.1 The “goal post” system used for ITP with agarose gel encapsulated electrolytes buffer system.

An investigation was carried out using an ITP with agarose encapsulated electrolytes buffer system for sodium ions. This simple electrolyte system was chosen for initial studies due to its ease of preparation.³⁹ In the early stage of investigation, a high concentration of sodium samples at 0.1 M was employed to determine the possibility of ions to migrate through the agarose gel and feasibility of ITP to operate under an agarose encapsulated electrolyte buffer system.

The system was set up as shown in Figure 3.1 where the syringe tube containing the agarose gel and electrolytes was connected in between two glass reservoirs forming a “goal post” system. 1 mL aliquots of LE buffer and 0.1 M NaCl in TE buffer were then introduced in reservoir A and B respectively. A high voltage of 1 kV was supplied for 30 min with the cathode (-ve) in A and anode (+ve) in B. Both samples from reservoirs A and B were diluted with Milli-Q water in 1:30 dilution and analysed for sodium ions using ICP-OES.

3.2.6 Preliminary investigation of ITP using agarose encapsulated electrolytes buffer system in a microfluidic chip

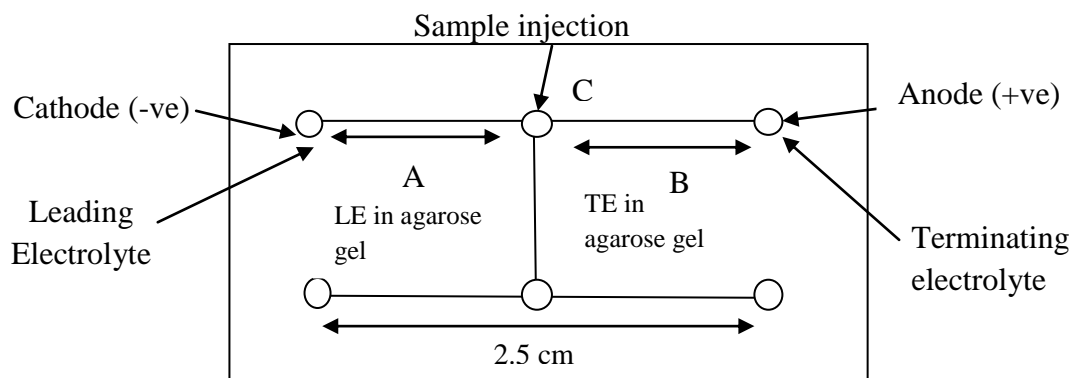


Figure 3.2 Schematic showing the design of microfluidic chip used for ITP (Channel diameter 104 μm , width 207 μm).

Preliminary investigation of ITP with an agarose encapsulated electrolytes buffer system in the microfluidic chip as shown in Figure 3.2 was conducted with the same procedure as described in section 3.2.5. The reservoir A was filled up with LE buffer, while reservoir B was filled up with TE buffer. 5 μl sample of 0.1 M NaCl was injected into the system through access hole C. A high voltage of 1 kV was supplied for 10 min.

3.3 Results and Discussion

3.3.1 Optimisation of the agarose gel rod containing leading and terminating electrolytes

3.3.1.1 Agarose gel concentration

Fabrication of an agarose gel rod containing two different sections of electrolytes was difficult as it required a certain viscosity to prevent both sections from mixing. A sufficient gel concentration is required to provide adequate viscosity but it must not be too high as this would significantly impede the ion migration. Agarose gel concentrations of 0.1%, 0.5%, 1% and 2% (w/v) were investigated to find the optimum concentration that had a balance between viscosity and ion migration.

Gel concentrations of 1% and 2% were shown to have sufficient viscosity and structural integrity to hold both electrolytes in position and prevent them from mixing when both electrolytes were introduced together. On the other hand, as the agarose gel concentrations of 0.1% and 0.5% were in a semi-liquid form, mixing of both electrolytes was observed due to insufficient viscosity. As a higher viscosity agarose gel matrix would impede the ion migration, an agarose gel concentration of 1% was chosen as the optimum for the fabrication of the agarose gel rod.

3.3.1.2 Resistance (Ω) of the agarose gel

As a high voltage was required for ITP to take place, the resistance (Ω) reading of the agarose gel rod and current (A) during experiment were investigated to make sure that the voltage supplied could meet the requirement. However, due to the constant voltage power supply which was used in the experiment, the current was limited to a maximum of 500 μ A. Therefore, according to Ohm's Law (Equation 3.1), the resistance of the system must be sufficiently high in order for the voltage to reach the requirement.

$$V(\text{voltage}) = I(\text{current}) \times R(\text{resistance}) \quad (\text{Equation 3.1})$$

As explained previously, this simple electrolyte buffer system reported by Prest *et al.* was chosen for the initial studies due to its ease of preparation.³⁹ Disappointingly, the average resistance of the 1% agarose gel rod containing 10 mM HCl with 0.1% HEC (LE) and 10 mM carnitine-HCl (TE) was only 15.8 kΩ which was very low. The voltage can be calculated using Ohm's Law as only 7.9 V. This means that the power supply could not reach the required voltage for ITP to take place; therefore the resistance of the system would need to be increased.

$$Resistance (\Omega) = Resistivity (\Omega m) \times \left(\frac{Length (m)}{Cross - sectional\ area (m^2)} \right)$$

(Equation 3.2)

According to the resistance equation stated in Equation 3.2, resistance of the agarose gel rod is dependent on three factors including the length of the tubes, cross-sectional area of the tubes and resistivity of the electrolytes in the tubes. As similar syringe tubes were used in the experiment, both the length and cross-sectional area of tube were fixed. Therefore, an increase in the resistivity of electrolytes would eventually increase the resistance of the agarose gel rod. Decreasing the concentration of the electrolytes causes a lesser amount of active species to ionise in the gel. This leads to lower conductivity which in turn increases the resistivity. An investigation was conducted by manipulating the concentration of the electrolyte buffer system in the agarose gel rod and the resistance reading were recorded in Table 3.1. As resistance is temperature-dependent, all agarose rods were kept at 4 °C prior to taking measurements to reduce the inaccuracy of the readings taken.

Table 3.1 Average resistance for agarose gel rod with different concentration of electrolytes. n=5

Experiment No.	Concentration of electrolytes		Average Resistance (kΩ)
	Leading Electrolyte	Terminating Electrolyte	
A	10 mM HCl + 0.1% HEC	10 mM Carnitine- HCl	15.8 ± 9.4%
B	5 mM HCl + 0.1% HEC	5 mM Carnitine- HCl	25.2 ± 11.3%

From the results depicted in Table 3.1, as expected, a higher resistance was recorded from the agarose gel rod in experiment B which contained half of the electrolyte concentration compared to experiment A. However, the difference in resistance observed between the two electrolyte concentrations was not significant. These results would indicate that the concentration of the electrolytes, in this case, had very little effect on the resistance of the agarose gel rod. Therefore, the original electrolyte concentrations as suggested by Prest *et al.* were used for further investigation.³⁹

3.3.2 Investigation of ITP using agarose encapsulated electrolytes buffer system in “goal post” system for sodium ions

An investigation as described in section 3.2.5 was carried out to determine the effect despite the resistance reading for the agarose gel being substantially low, causing the voltage supplied to be unable to meet the requirement for ITP. In order to compensate for the low voltage, a longer experimentation time was implemented, 30 min compared to 4 min reported by Prest *et al.*³⁹ Measurements of the sodium concentration within each buffer after the experiment were taken using ICP-OES and are documented in Table 3.2.

Table 3.2 The concentration of sodium in samples before and after isotachopheresis under condition of 1 kV for 30 min. n=1

Sample Contents	LE buffer 10 mM HCl + 0.1 % HEC (w/v)		TE buffer 10 mM Carnitine-HCl and 0.1 M NaCl	
	Before experiment	After experiment	Before experiment	After experiment
Sodium concentration in ppm	18.09	697.50	2288.89	1212.90
Sodium concentration in molarity (M)	0.787×10^{-3}	0.03	0.099	0.053

As can be seen from Table 3.2, a relationship was identified in which the amount of sodium ions in LE increased as the amount of sodium ions in TE decreased. The results obtained suggested that sodium ions were successfully migrated through the agarose encapsulated electrolyte buffer system during the experiment. However, it can clearly be seen that the concentration of sodium ions recovered was lower than the original concentration, which suggested that a certain amount of sodium ions were retained in the agarose gel tube. In order to investigate whether this may be the case, the resistance of the agarose gel rod was measured before and after the experiment and the readings are recorded in Table 3.3. The agarose gel rod after the experiment was kept at 4 °C overnight prior to taking measurements in order to eliminate any inaccuracy of measurement due to temperature changes.

Table 3.3 The resistance reading of the agarose gel rod before and after the ITP.

Resistance reading (kΩ) of	Before Experiment	After Experiment
the agarose gel rod	16.47	9.76

As shown in Table 3.3, there was a decrease in resistance reading of the agarose gel rod after the experiment. This can be explained by an increase in the amount of ionic species in the agarose gel, which is most likely to be the retained sodium ions.

The result obtained where sodium ions were successfully migrated through the gel encapsulated electrolyte buffer system offers the possibility of encapsulating the complex electrolyte system of ITP in agarose gel. This work was further expanded into a microfluidic chip in order to evaluate the feasibility of ITP taking place within the pre-loaded gels containing the electrolyte buffer system.

3.3.3 Miniaturised ITP in agarose encapsulated electrolytes buffer system in microfluidic chip.

As the cross-sectional area of the microfluidic chip was much smaller than the syringe tube, a higher resistance was achieved which in turn increased the voltage supplied in the system. Therefore, an investigation as described in section 3.2.6 was conducted where a shorter experimentation time of 10 min was applied.

However, the attempts of ITP in gel encapsulated electrolyte system in a microfluidic chip were unsuccessful as deformation of gel occurred soon after the experiment started. Numerous attempts were made to try and perform the ITP, but these were never successfully achieved. Such deformation of gel has been reported by Kondratova *et al.*, who explained that the phenomenon was caused by the heterogeneous electric field.^{94,95}

On the other hand, no adverse effects on the agarose gel were observed during the ITP in the “goal post” system, which may be due to the low voltage available in the system. Due to time constraints, no further investigation was carried out to overcome these problems.

3.3.4 Conclusion

Investigation of an ITP electrolyte buffer system encapsulated in agarose gel has been reported in this chapter. Initial studies in a “goal post” system have shown that sodium ions were successfully migrated through the gel encapsulated ITP electrolyte buffer system. This finding offers the potential to integrate an ITP buffer system in a microfluidic chip through agarose gel encapsulation for pre-concentration purposes.

Despite the demonstrated potential, the implementation of gel encapsulated ITP electrolyte buffer system into microfluidic chip was unsuccessful due to the occurrence of gel deformation. Previous reports in the literature explain that the gel deformation was caused by heterogenous electric field in the system.^{94,95} Further work would be required to overcome this problem so that further investigation on a gel encapsulation buffer system in microfluidic chip could be conducted. This would involve reducing the concentration of agarose gel or selecting an alternative medium.^{94,95}

Chapter 4

**Functionalisation of Silica Monoliths
for Ions Separation**

4.1 Introduction

As the ultimate aim of the whole project is to develop a μ TAS for *in situ* river water nutrients analysis, the separation column plays a vital role in the system. This chapter aims to investigate the possibility of developing an anion-exchange column through functionalisation with different ion exchangers on a self-fabricated silica monolithic column. As mentioned in chapter 1, a silica monolithic column was chosen over a packed column due to its low back pressure, tolerance to high flow rates, rapid and efficient chromatographic separations and high mechanical stability.⁶² Although a number of silica monolithic columns are available commercially, these silica columns are very expensive which contradicts the advantage of μ TAS. Therefore in order to be more cost-effective, a silica monolithic column was fabricated in-house via the sol-gel process based on the hydrolytic polycondensation of alkoxy silanes.⁷⁴

As the silica monoliths have a high content of silanol groups on the surface which facilitated functionalisation, various functional groups have been immobilised to fabricate ion exchange columns for chromatographic separation.⁶⁶ In this chapter, two different ion exchangers, chitosan and lysine are investigated for their possibility of immobilisation onto the self-fabricated silica monolith surface to develop anion exchange column. Chitosan and lysine are chosen for the immobilisation as they have been previously reported to be successfully immobilised onto a silica surface as well as having high content of amino functional groups which have the ability to retain anions under specific conditions.^{76,77,96} In the initial studies, a simple anion exchange solid phase extraction (SPE) experiment was conducted to evaluate the immobilisation of the ion exchangers based on their ability in retaining anions.

4.2 Experimental

4.2.1 Instrumentation

All anionic analysis was performed using DIONEX ICS 2000 system consisted of AS 11 HC 2 mm anion column (9 μm pore size), conductivity detection and KOH as the eluent.

4.2.2 Chemicals and Materials

Polyethylene oxide (average $M_v \sim 100,000$), nitric acid (HNO_3), tetraethoxysilane (TEOS), and ammonium hydroxide (NH_4OH) involved in the fabrication of sol-gel silica monolith were purchased from Sigma Aldrich (Dorset, UK). For the functionalisation of silica monolith, chitosan oligosaccharide lactate ($M_w \sim 5000$), 3-glycidoxypropyltrimethoxysilane (GPTMS), lysine, methanol, sodium dihydrogen phosphate (NaH_2PO_4), acetic acid, hydrochloric acid (HCL), sulphuric acid (H_2SO_4) were purchased from Sigma-Aldrich (Dorset, UK) whilst acetone, ethanol (EtOH), hydrogen peroxide (H_2O_2), and toluene were obtained from Fisher Scientific (Leicester, UK). Sodium acetate trihydrate and tris(hydroxymethyl) aminomethane (Tris) used to prepare the buffers were purchased from Fisher Scientific (Leicester, UK). Nitrate samples were made using sodium nitrate purchased from Sigma Aldrich (Dorset, UK). Milli-Q water used for all the experiments was purified by a Milli-Q system from Millipore Ltd (Livingston, UK) with a grade of 18 $\text{M}\Omega\cdot\text{cm}$ resistivity.

4.2.3 Fabrication of sol-gel TEOS silica monolith

The sol-gel TEOS silica monoliths were prepared according to a procedure similar to that described by Fletcher *et al.*⁷⁴ 0.28 g of polyethylene oxide (PEO) and a 0.29 mL aliquot of Milli-Q water were added to 2.54 mL of 1 M nitric acid and the mixture was stirred in an ice bath for ~20 min until a homogenous solution was formed. 2.26 mL of tetraethoxysilane (TEOS) was then added into the mixture and continuously stirred for 30 min in an ice bath to form a transparent solution. The solution was introduced into a plastic mould, tightly sealed and incubated at 40 °C in an oven for 3 days to allow the gelation process to form wet and semi-solid sol gel monoliths. The semi-solid monoliths were then washed with copious amounts of water to remove the residues, and treated with 10 times the volume of 1 M of NH₄OH at 85-90 °C for 24 h. The treated silica monoliths were washed with copious amounts of water again, and dried at 100 °C in an oven overnight. This was followed by the calcination step where the monoliths were heated at 550 °C for 6 h to remove the residual organic material. The silica monolith was then sealed within heat shrinkable Teflon tubing (Adtech Polymer Engineering Ltd, UK) at 320 °C to form a flow system (Figure 4.1).



Figure 4.1 In-house fabricated silica monolithic column sealed within Teflon tubing.

4.2.4 Functionalisation of silica monoliths with chitosan

The functionalisation of chitosan on silica monoliths was conducted as described by Cao *et al.*⁹⁶ with some modifications. Chitosan powder was dissolved in 10 mM acetic acid and 0.1% (w/v) (3-glycidopropyl)trimethoxysilane (GPTMS) through sonication for 30 min. GPTMS was added to act as the cross-linker between the silica monolith and chitosan. Optimisation of chitosan concentration was carried out by investigating a range of 1 to 4% (w/v) concentrations of chitosan.

Prior to functionalisation, the silica monoliths were cleaned in piranha solution (1 : 1, H₂SO₄ : H₂O₂) at 70 °C for 10 min, washed with copious amount of water and then dried with EtOH and acetone before putting in 100 °C oven for ~2 h or until completely dry. The purposes of cleaning in piranha solution were to remove organic residues and activate the surface of silica monoliths by exposing more hydroxyl groups.⁹⁷

The cleaned silica monoliths were then sealed with heat shrinkable tubes, and the chitosan solution was pumped through the monoliths overnight at a flow rate of 50 µl/h. The functionalised monoliths were then rinsed with 10 mM acetic acid to wash off the unbound chitosan, washed with water, EtOH, and acetone and dried in an oven at 100 °C for 2 h.

4.2.5 Functionalisation of silica monoliths with lysine

The procedure for functionalisation of lysine on silica monolith was adapted from the method described by Huang *et al.*⁷⁶ It was divided into 3 stages where the first stage was the addition of epoxy groups. A mixture of 2 mL GPTMS in 40 mL of dried toluene was prepared. The solution was pumped through the silica monolith at a flow rate of 0.1 mL/min for 1 h, and then the monolith was left at 100 °C in an oven for 1 h. This step was repeated three times and the final reaction was left overnight in the oven. The monolith was then washed with toluene and methanol.

The second stage was to create diol groups on the silica surface by opening the epoxy ring groups. The epoxy monolith was flushed with 0.1 mol/L hydrochloric acid with a flow rate of 1 mL/h for overnight and left at 100 °C oven for 2 h. The monolith was then washed with water and methanol.

The final stage was to immobilise lysine on the silica surface. Lysine solution was prepared by dissolving 1.46 g of lysine in 10 mL 50 mM NaH₂PO₄ with pH 8. The solution was then flowed through the monolith at flow rate of 1 mL/h for 1 h, and then reacted in a 100 °C oven for 1 h. This step was repeated twice and the final reaction was done overnight. The functionalised monolith was then washed with water and methanol.

4.2.6 Investigation of functionalised silica monolith as anion exchange column

In the preliminary investigation, experiments based on solid phase extraction (SPE) theory were conducted to evaluate the potential for immobilising chitosan or lysine onto the sol-gel fabricated silica monolith surface based on their ability in retaining anions. As successfully functionalised silica monoliths contain a high amount of pH-dependent amino groups (NH₂) on the surface, anions are bound to the positively charged protonated amino groups at low pH and released at a pH above the pK_a of the amino groups where deprotonation occurs.⁹⁷

For the protonation step, a pH 4 20 mM acetate buffer was prepared from sodium acetate trihydrate whereas for the deprotonation step, a pH 8.6 20 mM tris-acetate buffer was prepared from tris(hydroxymethyl) aminomethane (Tris) with the pH of both buffers being altered using acetic acid. Both buffers were prepared according to the Henderson-Hasselbach's equation (Equation 4.1).⁹⁸

$$\text{pH} = \text{pK}_a + \log_{10} \left(\frac{[\text{A}^-]}{[\text{HA}]} \right) \quad (\text{Equation 4.1})$$

The solid phase extraction method applied was adapted from the method outlined by Cao *et al.*⁹⁶ All the steps were performed at a flow rate of 10 $\mu\text{l}/\text{min}$. The initial step was to condition the column with activation buffer, 20 mM acetate buffer, pH 4 for 1 h. A 300 μl nitrate sample solution containing 5 mM NaNO_3 in 20 mM acetate buffer was then loaded into the silica monolith column. This was followed by the washing step where 20 mM acetate, pH 4 was flowed through for 1 h to wash off any unbound material. Elution was performed with 20 mM tris-acetate, pH 8.6 and all the eluent was collected in 300 μl aliquots for IC analysis. Similar procedure, buffers and sample were applied in both investigations of chitosan and lysine functionalised silica monoliths to allow relative comparison.

The percentage of nitrate ions recovered from each eluate was determined using Equation 4.2 in order to evaluate the extraction efficiency and retention ability of the functionalised silica monolith.

$$\text{Percentage of nitrate ions recovered (\%)} = \frac{\text{Peak area of nitrate recovered from each eluate } (\mu\text{S min})}{\text{Peak area of nitrate from sample } (\mu\text{S min})} \quad (\text{Equation 4.2})$$

4.3 Results and Discussion

4.3.1 Anion sample selection for investigation of functionalised silica monolith

The choice of anion sample for the preliminary investigation of functionalised silica monolith is crucial for optimum results. Nitrate ions were chosen as the anion samples for the investigation as nitrate is one of the most common contaminants found in river water. In addition, selection of nitrate as the anion sample increased the feasibility of anion retention by the functionalised silica monoliths as chitosan is well known for the extraction of nitrate ions present in water^{99,100}, while a lysine-functionalised column has been reported to have excellent ion-selectivity for nitrate.⁷⁶

4.3.2 Method selection for investigation of functionalised silica monolith

Solid phase extraction (SPE) rather than the anion chromatography separation method was chosen for the evaluation of immobilisation of the ion exchangers on the in-house silica monoliths column due to the simplicity of SPE. In addition, there was insufficient time for chromatography separation to be performed as the method required laborious work to determine a suitable eluent, flow rates, eluent concentration, and column length in order to achieve separation. On top of that, as the development of a miniaturised conductometric detection and suppressor system is still in progress, lack of a suitable detection system prevented the application of chromatographic separation.

SPE was suitable for the investigation as the amino groups (NH_2) on the surface of functionalised silica monolith are pH-dependent. Therefore, under low pH conditions, these amino groups were protonated into NH_3^+ which increased the electrostatic interaction between the positively charged amino groups and negatively charged anions leading to retention of the anions onto the surface of functionalised silica monolith. On the other hand, elution of anions from the functionalised silica surface occurred under high pH condition where the amino groups deprotonated causing the disruption in electrostatic interaction.

4.3.3 Analysis of the solid phase extraction buffer system

Solid phase extraction was carried out on an in-house fabricated monolithic silica column which had been functionalised. The success of the functionalisation process was confirmed using a commercial ion chromatography system to determine the amount of nitrate ions recovered after the SPE.

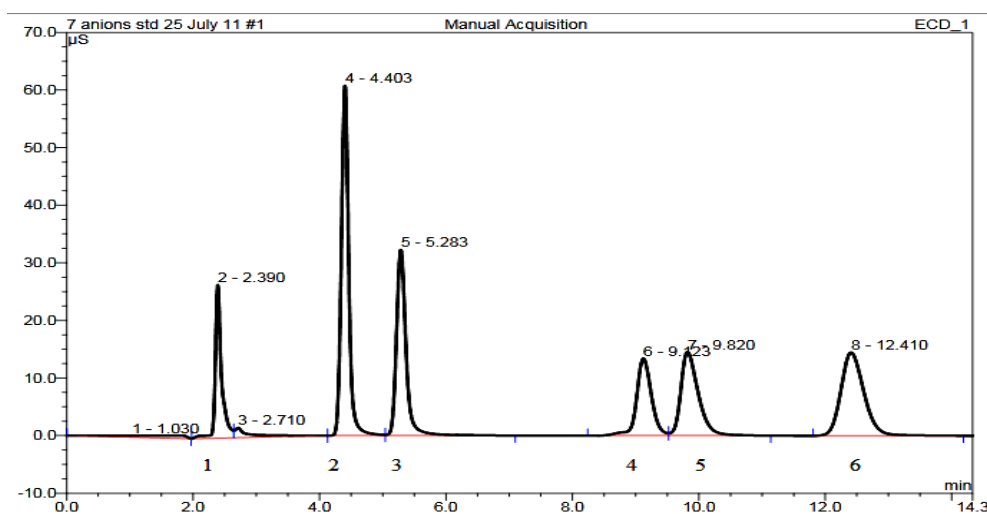


Figure 4.2 The chromatogram for 7 anions standard analysis obtained using Dionex IC. Peak 1= Fluoride, 2= Chloride, 3= Nitrite, 4= Nitrate, 5= Bromide, 6= Sulphate.

A standard analysis of 7 anions was carried out as a routine anion determination using a Dionex commercial column before running any experiments to make sure that the IC was operating properly. As can be seen from Figure 4.2, only six significant peaks were observed although 7 standard anions were analysed. This is because the 7th peak which corresponds to phosphate ions would only be released after 20 min due to its high retention.¹⁰¹ As phosphate ions were not of interest in the preliminary investigation, the elution of phosphate was not carried out in order to reduce the overall time for analysis. This result confirms that the IC was operating under appropriate conditions as all the peaks shown were fully resolved. In addition, the nitrate peak (peak 5) was shown to be fully resolved, confirming the efficiency and sensitivity of the IC system for determination of nitrate.

For both the chitosan and lysine functionalised silica columns, similar buffers and nitrate samples were used to allow relative comparison on the anion retention ability of both ion exchangers. IC analysis of the activation and elution buffers were carried out to determine the anions present in the buffer system. The ion chromatograms obtained are recorded in Figures 4.3 and 4.4.

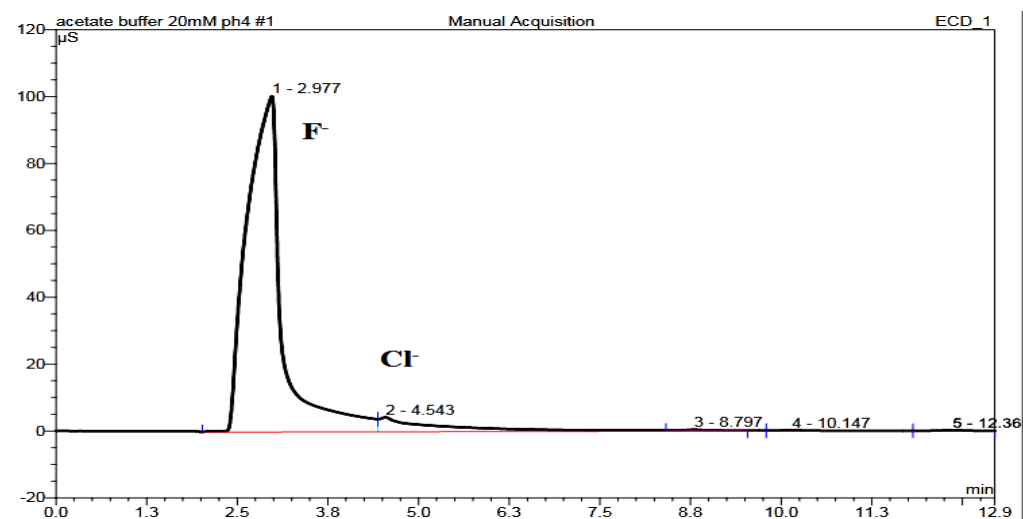


Figure 4.3 The ion chromatogram for the acetate buffer pH 4 (Activation buffer)

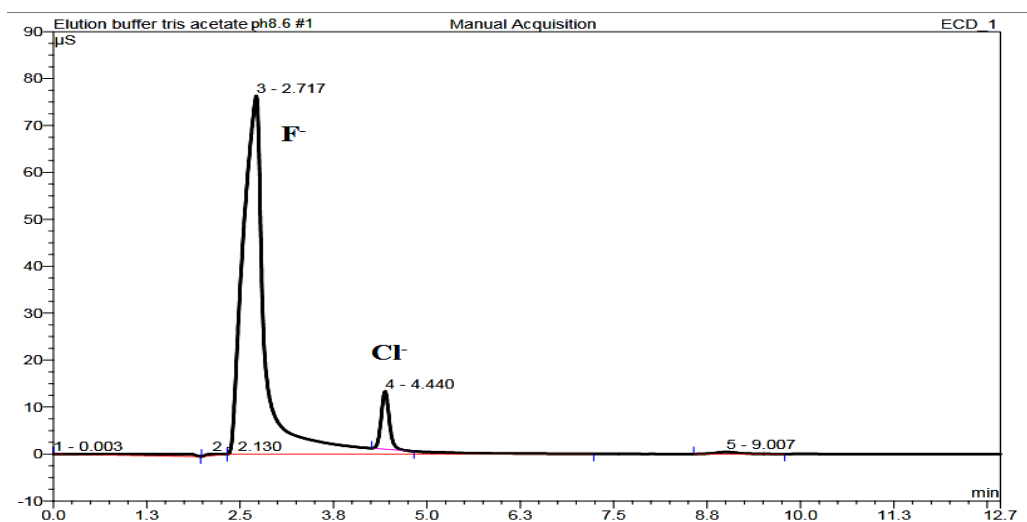


Figure 4.4 The ion chromatogram for the tris-acetate buffer pH 8.6 (Elution buffer)

As shown in Figures 4.3 and 4.4, the activation buffer and elution buffer used for the experiments contained insignificant amounts of nitrate. As nitrate ions were used as the sample for the investigation, these buffers were shown to provide minimal background noise for nitrate analysis. On the other hand, there are significant amount of fluoride ions present in both buffers which may interfere with nitrate ions for the binding site. This in turn reduces the nitrate binding capacity of the functionalised silica monolith. In order to overcome this issue, a high concentration of nitrate sample, 5 mM, was used to reduce the interference caused by other anions.¹⁰² IC analysis of the nitrate sample in acetate buffer was conducted to determine the anions present and the peak area of the nitrate ions.

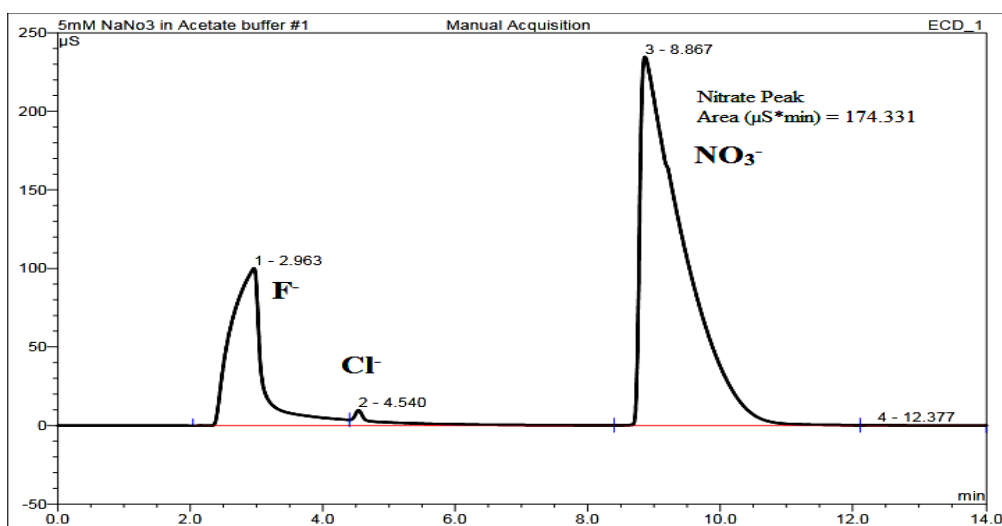


Figure 4.5 The ion chromatogram for the sample of 5mM NaNO₃ in acetate buffer

The ion chromatogram shown in Figure 4.5 indicates that the sample contained a much higher amount of nitrate ions compared to fluoride and chloride ions. As reported by Arora *et al.*, the high amount of nitrates reduces the interference from other anions while increasing the nitrate binding selectivity of the monoliths.¹⁰²

The peak area of nitrate ions in the sample was determined and used in further investigation to calculate the percentage of nitrate ions recovered after SPE on each functionalised silica monolith.

4.3.4 Investigation of solid phase extraction of nitrate ions by chitosan-functionalised silica monolith

4.3.4.1 Optimisation of chitosan concentration for functionalisation

Four batches of the chitosan-functionalised silica monolith prepared with different concentrations (1%, 2%, 3% and 4%) of chitosan were investigated to find the optimum concentration. Using higher concentration of chitosan for functionalisation provides a greater chance of binding onto the silica surface. It was, however, found that chitosan-functionalised silica monoliths prepared with 3% and 4% concentrations of chitosan were fully blocked and the only solution to unblock was to use a concentrated acid which would then disrupt the structure of silica monolith. A 2% chitosan concentration was therefore chosen to be the optimum concentration for the functionalisation.

4.3.4.2 Investigation of SPE using chitosan-functionalised silica monolith

Based on the experimental procedure as described in section 4.2.6, the experiments were performed using the chitosan-functionalised silica monolith and the recovery percentages of nitrate ions of each eluate fraction are summarised in Table 4.1.

Table 4.1 The recovery percentage of nitrate for each fraction during SPE. (n=1)

Peak area of initial nitrate sample = 174.331 μ S min

Fractions (Eluate volume : 300 μl)	Percentage of Nitrate ions Recovered (%)
1 (1 st washing)	14.8
2 (2 nd washing)	68.4
3 (1 st elution)	0.2
4 (2 nd elution)	0.1

As can be seen from Table 4.1, only a single set of data was successfully obtained due to insufficient time caused by the breakdown of the IC instrument. Although no appropriate conclusion can be drawn, the results showed approximately 83% of nitrate ions were recovered throughout the washing steps but less than 1% of nitrate ions were

recovered from the elution steps. This evidence suggested a negative result where most of the nitrate ions were washed off during the washing step instead of being retained by the chitosan-functionalised silica monolith. There are a few possible explanations for this, one of which is unsuccessful immobilisation of chitosan onto the silica surface due to poor cross-linking between the chitosan and the silica monolith.⁷⁷ Alternatively, it is possible that incomplete column pre-conditioning may be occurring, which then would require a longer conditioning time to allow protonation of the amino groups of the chitosan immobilised on the silica surface.

4.3.4.3 Investigation of SPE of nitrate ions by lysine-functionalised silica monolith

Immobilisation of lysine onto silica monolith and investigation of solid phase extraction using lysine-functionalised silica monolith were carried out in collaboration with a Chemistry PhD student, Asim Jilani. An experiment based on SPE procedure as described in section 4.2.6 was carried out and the percentage of nitrate ions recovered from each eluate fraction was determined and summarised in Table 4.2.

Table 4.2 The recovery percentage and standard deviation of nitrate for each fraction during SPE by lysine-functionalised silica monolith. (n=2) Peak area of initial nitrate sample=174.331 μ S min

Fractions (Eluate volume : 300 μ l)	Percentage of Nitrate ions Recovered (%)
1 (1 st washing)	2.9 \pm 1.1
2 (2 nd washing)	21.2 \pm 8.5
3 (1 st elution)	61.1 \pm 4.3
4 (2 nd elution)	1.2 \pm 0.9

As shown in Table 4.2, less than 25% of nitrate ions were washed off and approximately 62% of nitrate ions were successfully recovered from the elution steps. These results would indicate that the lysine was successfully immobilised onto the surface of silica monolith and had an average nitrate extraction efficiency of 62%. In addition, as can be seen by the standard deviation observed, the nitrate extraction efficiencies using lysine-functionalised silica monoliths exhibited a reasonable reproducibility. This is in agreement with several studies which suggested that the lysine bonded silica monolith possessed great reproducibility.^{73,76}

However, as a negative result was obtained from chitosan-functionalised silica monolith, no relative comparison can be made to evaluate the anion selectivity between the two ion exchangers. Even though only two sets of data were obtained from the investigation due to insufficient time caused by breakdown of the IC instrument, these findings suggested that lysine has the potential to be immobilised onto an in-house fabricated silica monolith surface to be an anion exchange separation column for the μ TAS.

4.3.5 Conclusion

This work has demonstrated the potential of fabricating an anion exchange column through functionalisation with an ion exchanger onto a self-fabricated silica monolithic column. Two ion exchangers, chitosan and lysine, were investigated and their success of immobilisation onto the silica monolithic surface was evaluated by SPE methodology. The lysine-functionalised self-fabricated silica monolith was shown to be capable of extracting nitrate ions with extraction efficiency of 62%. However, preliminary investigation of the chitosan-functionalised silica monolith was unsuccessful as most of the nitrate ions failed to be retained.

Further work is required to investigate the factors leading to the failure of nitrate retention by chitosan-functionalised silica monoliths. In addition, further work would be required to improve the results obtained, which involves optimising the experimental parameters and experimenting with other anions of interest.

Chapter 5

Conclusions and Future Work

Conclusions and Future Work

As part of the larger research effort towards developing a portable and automated μ TAS for *in situ* river water monitoring, this thesis aimed to develop an on-chip sample introduction system combined with sample filtration techniques. In addition, it also aimed to investigate the potential of ITP in an agarose gel encapsulated buffer system for on-chip sample pre-concentration, and fabrication of an anion exchange column using a self-fabricated silica monolithic column. From the results obtained in this thesis, a number of conclusions can be drawn from each chapter as outlined below.

5.1 The application of μ TAS for *in situ* river water monitoring

In the early part of chapter 1, the importance of *in situ* high frequency surface water monitoring was discussed. The section focused on the problems encountered by the current conventional monitoring techniques and the advantages of μ TAS in the development of a portable and automated *in situ* monitoring system.

The two main sample introduction techniques for μ TAS, namely, electrokinetic injection and hydrodynamic injection presented in the current literature were discussed. It was found that although no electrokinetic bias is present in the sample introduced through hydrodynamic injection, the main disadvantage of hydrodynamic flow is the requirement of mechanical moving parts. The integration of on-chip injectors and valves needed for hydrodynamic injection greatly reduces the portability of μ TAS. On the other hand, electrokinetic injection has proved to be substantially more suitable for the applications within this thesis as it involves only a number of electrodes imbedded in the μ TAS, and there is better and easier control of the sample flow.

The advantages of sample pre-treatment techniques in microfluidic systems, including sample filtration and sample pre-concentration of river water, were evaluated. The current literature on sample filtration techniques was reviewed and it was concluded that a structurally-based filter (frit) would be studied further due to its ease of preparation

and because it has been demonstrated to successfully remove particulates that cause system blockage. In addition, the three most common sample pre-concentration techniques were discussed and ITP was chosen specifically for its high concentration enhancement factor.

In the latter part of chapter 1, the background, mechanism, theory and application of ion chromatography were discussed including the ion exchange principle for the separation process. The advantages and disadvantages of both silica and organic polymer monolithic separation columns were evaluated and it was concluded that a silica monolithic column was more appropriate for this thesis due to high chromatographic efficiency and availability of various potential post-modifications.

5.2 On-chip sample introduction system with filtration mode

In chapter 2, the work presented a detailed evaluation of a sample introduction system coupled with sample filtration performed on a microfluidic device. A potassium silicate frit was successfully fabricated within the microfluidic chip and the precise placement of the frit was achieved using a highly viscous glycerol solution which restricted the movement of the frit. Optimisation of the potassium silicate frit was carried out by assessing several factors including the frit composition ratio, incubation time and oven temperature. The frit fabricated by the optimised protocol was proven to possess high mechanical stability and flow resistance against hydrodynamic and hydrostatic flow. Electrokinetic injection was used to introduce sodium ions into the microfluidic chip through the potassium silicate frit. EOF suppression was achieved through dynamic coating by using 0.5% (w/v) HEC in order to allow only electrophoretic flow in the system. Sodium ions were shown to successfully migrate through the high flow resistance potassium silicate frit by electrophoretic flow with ion migration efficiency of 26%. The ion migration was validated by a diffusion test which showed that the migration of sodium ions was purely due to electrophoretic flow. Despite the low ion migration efficiency obtained, the results showed the possibility of integrating a sample filtration frit within the sample introduction system which allowed the analyte ions to be selectively extracted from the sample matrix.

The custom-made prototype contactless conductivity detector was evaluated for its sensitivity in determining conductivity changes within the sample introduction system during ion migration. Even though peak broadening was observed, the prototype was shown to be capable of detecting conductivity changes which allowed real-time monitoring to make sure that the sample introduction system is functioning properly.

In order to further improve the work presented, further work would include silanisation of the frit and optimisation of factors such as voltage and experimentation time to increase the ion migration efficiency. While the focus of this study has been on sodium ions, there are a wide variety of cations and anions of interest which can be investigated to determine their potential problems during sample introduction through the frit. Further work is required to increase the sensitivity of the contactless detector and reduce the influences of other factors such as temperature before implementation onto a microfluidic chip.

5.3 Sample pre-concentration with miniaturised isotachopheresis

Chapter 3 focused on the encapsulation of an ITP electrolyte buffer system in agarose gel to allow timely and cost-effective introduction of the buffer system into a microfluidic chip. A proof of principle experiment was carried out in a “goal-post” system to investigate the feasibility of ITP taking place within an agarose encapsulated electrolyte buffer system environment. Optimisation of agarose gel concentration was conducted so that sufficient viscosity to prevent mixing of both electrolytes could be obtained. An ITP process was investigated on the agarose gel encapsulated electrolytes buffer in a “goal post” system and it was shown that sodium ions successfully migrated through the gel encapsulated buffer system. Despite the demonstrated potential of encapsulating the buffer system in agarose gel, the attempt to conduct ITP within gel encapsulated buffers in microfluidic chip was unsuccessful due to the occurrence of gel deformation. Further work would be required to solve the gel deformation issue, which would involve reducing the concentration of agarose gel or opting for an alternative medium.

5.4 Functionalisation of silica monoliths for ions separation

Chapter 4 describes the successful fabrication of a silica monolithic column via the sol-gel method and functionalisation of the silica monolith with ion exchanger to produce an anion exchange column. The work presented has demonstrated the potential of fabricating an anion exchange column through functionalisation with an ion exchanger onto a self-fabricated silica monolithic column, which is more cost-effective than commercial silica columns. Two different ion exchangers, chitosan and lysine, were investigated and the SPE method was used to evaluate the success in immobilisation of the ion exchangers onto the silica surface based on their anion retention ability. Lysine was successfully immobilised onto the fabricated silica monolith and found to be capable of retaining nitrate ions with extraction efficiency of 62%. On the other hand, nitrate ions were not retained by the chitosan functionalised silica monolith, which might be due to poor cross linking or incomplete column pre-conditioning.

Further work is required in order to improve the results obtained. Investigation of the reproducibility of both functionalised silica monoliths should be conducted to produce better results. Further work would also be required to investigate the factors causing failure of nitrate retention by the chitosan functionalised silica monolith. In addition, while the focus of the work has been on SPE, a further work would be the investigation of anion exchange columns through anion chromatographic separation.

Chapter 6 References

1. <http://water.epa.gov/drink/contaminants/index.cfm#List> Accessed on July 2012.
2. G.D. Liu, W.L. Wu and J. Zhang, *Agric. Ecosyst. Environ.*, 2005, **107**, 211.
3. L. Fewtrell, *Environ. Health Perspect.*, 2004, **14**, 1371.
4. G. Arhonditsis, M. Eleftheriadou, M. Karydis and G. Tsirtsis, *Mar. Pollut. Bull.*, 2003, **46**, 1174.
5. N. Berenzen, R. Schulz and M. Liess, *Water Res.*, 2001, **35**, 3478.
6. J.S. Horsburgh, A.S. Jones, D.K. Stevens, D.G. Tarboton and N.O. Mesner, *Environ. Modell. Softw.*, 2010, **25**, 1031.
7. J.C. Seiter and M.D. DeGrandpre, *Talanta*, 2001, **54**, 99.
8. A. Laš, R. Vuillemin, B. Leilde, G. Sarthou, C. Bournot-Marec and S. Blain, *Mar. Chem.*, 2005, **97**, 347.
9. A. Ayala, L.O. Leal, L. Ferrer and V. Cerda, *Microchem. J.*, 2012, **100**, 55.
10. A. Jang, Z. Zou, K. K. Lee, C.H. Ahn and P.L. Bishop, *Meas. Sci. Technol.*, 2011, **22**, Doi:10.1088/0957-0233/22/3/032001.
11. A.D. Beaton, V.J. Sieben, C.F.A. Floquet, E.M. Waugh, S.A.K. Bey, I.R.G. Ogilvie, M.C. Mowlem and H. Morgan, *Sens. Actuators B*, 2011, **156**, 1009.
12. L. Marle and G.M. Greenway, *Trends Anal. Chem.*, 2005, **24**, 795.
13. S.C. Terry, J.H. Jerman and J.B. Angell, *IEEE Trans. Electron Devices*, 1979, **26**, 1880.
14. A. Manz, N. Graber and H.M. Widmer, *Sens. Actuators*, 1990, **B1**, 244.
15. H. Yang and R.L Chien, *J. Chromatogr. A*, 2001, **924**, 155.
16. C.C. Lin, J.L. Hsu and G.B. Lee, *Microfluid. Nanofluid.*, 2011, **10**, 481.
17. A.G. Crevillén, M. Hervás, M.A. López, M.C. González, and A. Escarpa, *Talanta*, 2007, **74**, 342.
18. A. Rós, A. Escarpa, M.C. González and A.G. Crevillén, *Trends Anal. Chem.*, 2006, **25**, 467.

19. P.A. Greenwood and G.M. Greenway, *Trends Anal. Chem.*, 2002, **21**, 726.
20. G.J.M. Bruin, *Electrophoresis*, 2000, **21**, 3931.
21. D.W. Kim and S.H. Kang, *J. Chromatogr. A*, 2005, **1064**, 121.
22. S.J. Haswell, *Analyst*, 1997, **122**, 1R.
23. J. A. Oakley, Ph.D. Thesis, University of Hull, 2009.
24. M. Schlund, S.E. Gilbert, S. Schnydrig and P. Renaud, *Sens. Actuators B*, 2007, **123**, 1133.
25. D.R. Baker, *Capillary Electrophoresis*, John Wiley & Sons, New York, 1995.
26. P. Coufal, K. Stulik, H.A. Claessens and C.A. Cramers, *J. High Resolut. Chromatogr.*, 1994, **17**, 325.
27. B. Gaš, *Electrophoresis*, 2009, **30**, S7.
28. P.M. Flanigan, D. Ross and J.G. Shackman, *Electrophoresis*, 2010, **31**, 3466.
29. http://www.aesociety.org/areas/microchip_electrophoresis_body.php
Accessed on July 2012.
30. J. Lichtenberg, N.F.D. Rooij and E. Verpoorte, *Talanta*, 2002, **56**, 233.
31. A.J. de Mello and N. Beard, *Lab Chip*, 2003, **3**, 11N.
32. R. Bodor, V. Madajov á D. Kaniansky, M. Mas á, M. J čnck and B. Stanislawski, *J. Chromatogr. A*, 2001, **916**, 155.
33. B. He, L. Tan and F. Regnier, *Anal. Chem.*, 1999, **71**, 1464.
34. J.P. Brody and P. Yager, *Sens. Actuators A*, 1997, **58**, 13.
35. K. Sueyoshi, F. Kitagawa and K. Otsuka, *J. Sep. Sci.*, 2008, **31**, 2650.
36. C.J. Holloway and I. Trautschold, *Fresenius J. Anal. Chem.*, 1982, **311**, 81.
37. http://physicalchemistryresources.com/Book4_sections/pc_is_titleandcontents_08222010.htm Accessed on July 2012.

38. D. Liu, M. Shi, H. Huang, Z. Long, X. Zhou, J. Qin and B. Lin, *J. Chromatogr. B*, 2006, **844**, 32.
39. J.E. Prest, S.J. Baldock, N. Bektas, P.R. Fielden and B.J.T. Brown, *J. Chromatogr. A*, 1999, **836**, 59.
40. S. J. Baldock, P.R. Fielden, N.J. Goddard, H.R. Kretschmer, J.E. Prest and B.J.T. Brown, *Microelectron. Eng.*, 2008, **85** 1440.
41. M. Mas á, M. Dankov á E. Ölveck á A. Stachurov á D. Kaniansky and B. Stanislawski, *J. Chromatogr. A*, 2004, **1026**, 31.
42. J.E. Prest, M.S. Beardah, S.J. Baldock, S.P. Doyle, P.R. Fielden, N.J. Goddard and B.J.T. Brown, *J. Chromatogr. A*, 2008, **1195**, 157.
43. J.E. Prest and P.R. Fielden, *Talanta*, 2008, **75**, 841.
44. L. Chen, J.E. Prest, P.R. Fielden, N.J. Goddard, A. Manz and P.J.R. Day, *Lab Chip*, 2006, **6**, 474.
45. J.P. Kutter, S.C. Jacobson and J.M. Ramsey, *J. Microcolumn Sep.*, 2000, **12**, 93.
46. J. Liu, C.F. Chen, C.W. Tsao, C.C. Chang, C.C. Chu and D.L. DeVoe, *Anal. Chem.*, 2009, **81**, 2545.
47. Y. Yang, C. Li, K.H. Lee and H.G. Craighead, *Electrophoresis*, 2005, **26**, 3622.
48. J.P. Murrphy, M.C. Breadmore, A. Tan, M. McEnery, J. Alderman, C. O'Mathuna, A.P. O'Neill, P. O'Brien, N. Advoldvic, P.R. Haddad and J.D. Glennon, *J. Chromatogr. A*, 2001, **924**, 233.
49. J. Cleary, C. Slater and D. Diamond, *International Journal of Civil and Environmental Engineering*, 2010, **2**, 145.
50. Q. Kang, N.C. Golubovic, N.G. Pinto and H.T. Henderson, *Chem. Eng. Sci.*, 2001, **56**, 3409.
51. B.A. Adams and E.L. Holmes, *J. Soc. Chem. Ind.*, 1935, **54**, 1T.
52. H. Small, T.S. Stevens and W.C. Bauman, *Anal. Chem.*, 1975, **47**, 1801.

53. http://media.wiley.com/product_data/excerpt/19/35272870/3527287019.pdf
Accessed on July 2012.
54. H. Small, *Modern Analytical Chemistry: Ion Chromatography*, Plenum Press, New York, 1989.
55. P.R. Haddad and P.E. Jackson, *Ion Chromatography: Principles and Applications*, Elsevier, New York, 1990.
56. J. Weiss, *Ion Chromatography*, 2nd Edition, VCH, Weinheim, 1995.
57. R. Garc ía-Fern ández, J.I. Garc ía-Alonso and A. Sanz-Medel, *J. Chromatogr. A*, 2004, **1033**, 127.
58. M. Neal, C. Neal, H. Wickham and S. Harman, *Hydrol. Earth Syst. Sci.*, 2007, **11**, 294.
59. B. Paull and P.N. Nesterenko, *Trends Anal. Chem.*, 2005, **24**, 295.
60. K.M. Glenn, C.A. Lucy and P.R. Haddad, *J. Chromatogr. A*, 2007, **1155**, 8.
61. F. Svec and J.M.J. Fr échet, *J. Chromatogr. A*, 1995, **702**, 89.
62. S. Constantin and R. Freitag, *J. Sol-Gel Sci. Technol.*, 2003, **28**, 71.
63. M.Y. Ding, R. Zheng and H. Peng, *Chin. J. Anal. Chem.*, 2009, **37**, 395.
64. J.P. Hutchinson, E.F. Hilder, M. Macka, N. Avdalovic and P.R. Haddad, *J. Chromatogr. A*, 2006, **1109**, 10.
65. D. Schaller, E.F. Hilder and P.R. Haddad, *J. Sep. Sci.*, 2006, **29**, 1705.
66. F. Zhang, Y. Li, Z. Guo, T. Liang, B. Yang, Y. Zhou and X. Liang, *Talanta*, 2011, **85**, 112.
67. K. Nakanishi, *J. Porous Mater.*, 1997, **4**, 67.
68. P. Hatsis and C.A. Lucy, *Analyst*, 2002, **127**, 451.
69. P. Hatsis and C.A. Lucy, *Anal. Chem.*, 2003, **75**, 995.
70. D. Connolly, D. Victory and B. Paull, *J. Sep. Sci.*, 2004, **27**, 912.
71. D. Victory, P. Nesterenko and B. Paull, *Analyst*, 2004, **129**, 700.

72. E. Sugrue, P. Nesterenko and B. Paull, *Analyst*, 2003, **128**, 417.
73. E. Sugrue, P. Nesterenko and B. Paull, *J. Chromatogr. A*, 2005, **1075**, 167.
74. P.D.I. Fletcher, S.J. Haswell, P. He, S.M. Kelly and A. Mansfield, *J. Porous Mater.*, 2011, **18**, 501.
75. H. Minakuchi, K. Nakanishi, N. Soga and N.J. Tanaka, *J. Chromatogr. A*, 1997, **762**, 135.
76. G. Huang, Q. Lian, W. Zeng and Z. Xie, *Electrophoresis*, 2008, **29**, 3896.
77. Z. Lu, P. Zhang and L. Jia, *J. Chromatogr. A*, 2010, **1217**, 4958.
78. B. Behnke, E. Grom and E. Bayer, *J. Chromatogr. A*, 1995, **716**, 207.
79. P.H. Petsul, G.M. Greenway and S.J. Haswell, *Anal. Chim. Acta*, 2001, **428**, 155.
80. P.D. Christensen, S.W.P. Johnson, T. McCreedy, V. Skelton and N.G. Wilson, *Anal. Commun.*, 1998, **35**, 341.
81. S.M. Piraino and J.G. Dorsey, *Anal. Chem.*, 2003, **75**, 4292.
82. K.J. Shaw, Ph.D. Thesis, University of Hull, 2009.
83. E.N. Fung, H. Pang and E.S. Yeung, *J. Chromatogr. A*, 1998, **806**, 157.
84. K.A. Snyder and J. Marchand, *Cem. Concr. Res.*, 2001, **31**, 1837.
85. R.F.S. Lenza, and W.L. Vasconcelos, *Mater. Res.*, 2001, **4**, 175.
86. Q.S. Qu, Y.Z. He, W.E. Gan, N. Deng and X.Q. Lin, *J. Chromatogr. A*, 2003, **983**, 255.
87. D. Belder and M. Ludwig, *Electrophoresis*, 2003, **24**, 3595.
88. J. Horvath and V. Dolnik, *Electrophoresis*, 2001, **22**, 644.
89. H. Tian and J.P. Landers, *Anal. Biochem.*, 2002, **309**, 212.
90. C.Y. Liu, X. Xu and J.R. Chen, *Can. J. Anal. Sci. Spectros.*, 2008, **53**, 171.
91. M.A. Hayes, I. Kheterpal and A.G. Ewing, *Anal. Chem.*, 1993, **65**, 27.

92. B.R. Reschke, J. Schiffbauer, B. F. Edwards and A.T. Timperman, *Analyst*, 2010, **135**, 1351.
93. J.A. Oakley, K.J. Shaw, P.T. Docker, C.E. Dyer, J. Greenman, G.M. Greenway and S.J. Haswell, *Lab Chip*, 2009, **9**, 1596.
94. V.N. Kondratova, I.V. Botezatu, V.P. Shelepov and A.V. Lichtenstein, *Biochem. (Moscow)*, 2009, **74**, 1285.
95. V.N. Kondratova, O. I. Serd'uk, V.P. Shelepov and A.V. Lichtenstein, *BioTechniques*, 2005, **39**, 695.
96. W. Cao, C.J. Easley, J.P. Ferrance and J.P. Landers, *Anal. Chem.*, 2006, **78**, 7222.
97. K.A. Hagan, W.L. Meier, J.P. Ferrance and J.P. Landers, *Anal. Chem.*, 2009, **81**, 5249.
98. <http://www.chemteam.info/AcidBase/HH-Equation.html>
Accessed on August 2012.
99. S. Chatterjee and S.H. Woo, *J. Hazard. Mater.*, 2009, **164**, 1012.
100. S. Chatterjee, D.S. Lee, M.W. Lee and S.H. Woo, *J. Hazard. Mater.*, 2009, **166**, 508.
101. http://www.dionex.com/en-us/webdocs/4157-PS-Dionex-IonPac-AS11-AS11-HC-28Mar2012-PS70024_E.pdf
Accessed on September 2012.
102. M. Arora, N.K. Eddy, K.A. Mumford, Y. Baba, J.M. Perera and G.W. Stevens, *Cold Reg. Sci. Technol.*, 2010, **62**, 92.